HYPERBOLIC BALANCE LAWS: RIEMANN INVARIANTS AND THE GENERALIZED RIEMANN PROBLEM

MATANIA BEN-ARTZI AND JIEQUAN LI

Abstract. The Generalized Riemann Problem (GRP) for nonlinear hyperbolic system of m balance laws (or alternatively "quasi-conservative" laws) in one space dimension is formulated as follows: Given initial-data which are analytic on two sides of a discontinuity, determine the time evolution of the solution at the discontinuity. In particular, the GRP numerical scheme (second-order high resolution) is based on an analytical evaluation of the first time derivative. The analytical solution is readily obtained for a single equation ($m = 1$) and, more generally, if the system is endowed with a complete (coordinate) set of Riemann invariants. In this case it can be "diagonalized" and reduced to the scalar case. However, most systems with $m > 2$ do not admit such a set of Riemann invariants. This paper introduces a generalization of this concept: "Weakly Coupled Systems" (WCS). Such systems have only "partial set" of Riemann invariants, but these sets are weakly coupled in a way which enables a "diagonalized" treatment of the GRP. An important example of a WCS is the Euler system of compressible, nonisentropic fluid flow ($m = 3$). The solution of the GRP discussed here is based on a careful analysis of rarefaction waves. A "propagation of singularities" argument is applied to appropriate Riemann invariants across the rarefaction fan. It serves to "rotate" initial spatial slopes into "time derivative". In particular, the case of a "sonic point" is incorporated easily into the general treatment. A GRP scheme based on this solution is derived, and several numerical examples are presented. Special attention is given to the "acoustic approximation" of the analytical solution. It can be viewed as a proper linearization (different from the approach of Roe) of the nonlinear system. The resulting numerical scheme is the simplest (second-order, high-resolution) generalization of the Godunov scheme.

Key words: Hyperbolic balance laws, Generalized Riemann problem (GRP) scheme, Riemann invariants, Godunov scheme, MUSCL-type schemes, G_∞-scheme, G_1-scheme, weakly coupled systems.

AMS subject classification 2000: Primary: 65M06, 35L60; Secondary: 35L65, 76M20.

Contents

1. Introduction

In this paper we consider the generalized Rieman problem (GRP) for hyperbolic balance laws

$$\frac{\partial U}{\partial t}+\frac{\partial F(U)}{\partial x}=S(x,U), \tag{1.1}$$

where $U=(u_1,\cdots,u_m)^\top$ is an unknown function of x and t, $F=(f_1,\cdots,f_m)^\top$ is the associated flux, and $S(x,U)$ is the source term resulting from geometrical and physical effects. We develop the method of Riemann invariants in order to solve the generalized Riemann problem and derive a GRP high resolution scheme for the system. Our starting point in the present study is the associated Riemann problem, i.e., the Riemann problem for the homogeneous counterpart of (1.1), which is assumed to be solvable theoretically and numerically. We show that the Riemann invariants, which always exist for strictly hyperbolic systems of two equations (i.e., $m=2$), play a pivotal role in the GRP solution for a large family of hyperbolic systems, including the system of shallow water equations, the compressible fluid flow (both isentropic and non-isentropic) and so on.

The GRP scheme was originally designed for compressible fluid flows [1, 4]. As the extension of the Godunov scheme [9], the GRP scheme assumes piecewise initial data and evolves the solution of (1.1) by analytically solving the generalized Riemann problem at each cell interface with second order accuracy. Specifically, we denote by $C_j=[x_{j-1/2},x_{j+1/2}]$ ($\Delta x=x_{j+1/2}-x_{j-1/2}$) the computational cell numbered j, and by $\{t_n\}_{n=0}^{\infty}$ the sequence of discretized time levels, $\Delta t=t_{n+1}-t_n$. Assume that the data at time $t=t_n$ is piecewise linear with a slope σ_j^n, i.e. on C_j we have

$$U(x,t_n)=U_j^n+\sigma_j^n(x-x_j),\quad x\in(x_{j-1/2},x_{j+1/2}). \tag{1.2}$$

Then a Godunov-type scheme of second order usually takes the form

$$U_j^{n+1} = U_j^n - \frac{\Delta t}{\Delta x}\left(F_{j+1/2}^{n+1/2} - F_{j-1/2}^{n+1/2}\right) + \frac{\Delta t}{2}\left(S_{j+1/2}^{n+1/2} + S_{j-1/2}^{n+1/2}\right), \tag{1.3}$$

where we use the notations

$$F_{j+1/2}^{n+1/2} = F(U_{j+1/2}^{n+1/2}), \quad S_{j+1/2}^{n+1/2} = S(x_{j+1/2}, U_{j+1/2}^{n+1/2}), \tag{1.4}$$

and U_j^n is the average of $U(x,t_n)$ over the cell C_j and $U_{j+1/2}^{n+1/2}$ is the mid-point value or the average of $U(x_{j+1/2},t)$ over the time interval $[t_n,t_{n+1}]$. The source term $S(x,U)$ is currently discretized with an interface method, which is the trapezoidal rule in space and the mid-point rule in time [4, 11]. The central issue is how to obtain the mid-point value $U_{j+1/2}^{n+1/2}$. The GRP scheme formally approximates this value by the Taylor expansion (ignoring higher order terms),

$$U_{j+1/2}^{n+1/2} \cong U_{j+1/2}^n + \frac{\Delta t}{2}\left(\frac{\partial U}{\partial t}\right)_{j+1/2}^n, \tag{1.5}$$

where

$$U_{j+1/2}^n = \lim_{t\to t_n+0} U(x_{j+1/2},t), \quad \left(\frac{\partial U}{\partial t}\right)_{j+1/2}^n = \lim_{t\to t_n+0}\frac{\partial U}{\partial t}(x_{j+1/2},t). \tag{1.6}$$

The value $U_{j+1/2}^n$ is obtained by solving the associated Riemann problem for the homogeneous hyperbolic conservation laws as used in the first order Godunov scheme [9]. We are left with the calculation of $(\partial U/\partial t)_{j+1/2}^n$, which is the main ingredient in the GRP solution.

Let us take a look at a single equation case (U, F in (1.1) are scalar functions). At each grid point $(x_{j+1/2},t_n)$, only a single wave emanates. Therefore we are able to use the equation (1.1) to get

$$\left(\frac{\partial U}{\partial t}\right)_{j+1/2}^n = -F'(U_{j+1/2}^n)\cdot\left(\frac{\partial U}{\partial x}\right)_{j+1/2}^n + S(x_{j+1/2},U_{j+1/2}^n), \tag{1.7}$$

where $(\partial U/\partial x)_{j+1/2}^n$ is upwind taken from the initial data at time $t=t_n$. That is, $(\partial U/\partial x)_{j+1/2}^n$ is taken from the left (resp. right) hand side of $x = x_{j+1/2}$ if $F'(U_{j+1/2}^n) > 0$ (resp. $F'(U_{j+1/2}^n) < 0$). It is clear that the limiting value $(\partial U/\partial t)_{j+1/2}^n$ does not vanish due to the source term effect even if initially the slopes σ_j^n in (1.2) are identically zero. Therefore even in the first order Godunov scheme the time derivative $(\partial U/\partial t)_{j+1/2}^n$ should be properly treated.

In general (1.7) is not valid when (1.1) is a system, because there exists more than one nonlinear wave issuing from the singularity point $(x_{j+1/2},t_n)$ and the interface $x = x_{j+1/2}$ is, generally speaking, located in an intermediate region. We are therefore looking for the substitute of (1.7) in the system case. As a motivation for our treatment, consider the following strictly linear hyperbolic system,

$$\frac{\partial U}{\partial t} + A\frac{\partial U}{\partial x} = 0, \tag{1.8}$$

where A is a constant matrix with m real distinct eigenvalues. Denote by Λ the diagonal matrix whose entries are the eigenvalues of A, and by L the matrix whose row vectors are

the left eigenvectors of A. Then the standard diagonalization process yields

$$\frac{\partial W}{\partial t} + \Lambda \cdot \frac{\partial W}{\partial x} = 0, \qquad W = LU. \tag{1.9}$$

These equations are entirely decoupled, each component of W can be treated as in the scalar case.

For the nonlinear case we have similar conclusions when the system (1.1) is endowed with a coordinate system of Riemann invariants [8]. An important and direct consequence is that (1.1) can be transformed into a weakly coupled form, analogous to the linear case mentioned above. Moreover in the associated Riemann problem the Riemann invariants are constant throughout the corresponding rarefaction wave, or in the linearly degenerate case they are continuous across the corresponding contact discontinuity. These properties have the following implications:

(i) Thinking of the initial data (1.2) with non-zero slopes as a perturbation of piecewise constant Riemann initial data and the source term $S(x, U)$ as a perturbation of the homogeneous system of equations, the solution of the generalized Riemann problem for (1.1) is a perturbation of the solution of the associated Riemann problem mentioned above at least in the neighborhood of the singularity point. Therefore the Riemann invariants are regular locally across the corresponding (curved) rarefaction wave (in the generalized Riemann problem) although the derivatives of the solution of (1.1) usually explode there. Thus we can take a usual calculus manipulation for the Riemann invariants.

(ii) Each Riemann invariant is transported with a single equation (see Theorem 4.3). The transport equation enables us to resolve the rarefaction wave in a quite simple way, analogous to the treatment of the scalar equation. Certainly we need to overcome the technical coupling difficulty by using characteristic coordinates. In this paper, we use the Riemann invariants to resolve the rarefaction waves in the generalized Riemann problem for (1.1) as a main ingredient in our GRP solution.

(iii) The fact that the Riemann invariants are continuous across the corresponding contact discontinuity simplifies the resolution of contact discontinuities.

(iv) The existence of Riemann invariants is independent of the Eulerian or Lagrangian formulation of physical models. Therefore, the resulting schemes could be either Eulerian or Lagrangian. We avoid the passage from the Lagrangian version to the Eulerian case, as was done in [1].

(v) In each rarefaction wave, the behavior of the corresponding Riemann invariant is determined by a suitable (scalar) transport equation. As a consequence, the sonic case, i.e., when the rarefaction wave spans the cell interface, is automatically resolved, see Subsections 6.1 and 7.2. Recall that the sonic case is the most delicate in the original GRP scheme [1] or MUSCL-type schemes.

Therefore it is natural to use the Riemann invariants to solve the generalized Riemann problem and derive the resulting GRP scheme. This idea has been used in the context of shallow water equations and planar compressible fluid flows [13, 5]. As is well-known [8, Sec. 7.3], any strictly hyperbolic system of two equations is endowed with a coordinate system of Riemann invariants. On the other hand, such a coordinate system does not generally exist for systems of the form (1.1) when $m \geq 3$. However, many physical systems are weakly coupled (in a sense to be made precise later, see Definition 7.7) and can be reduced into a

form that is amenable to the Riemann invariant approach. In particular, we can use this approach to handle the system of compressible fluid duct flows in Section 9.

Next we point out the difference between our approach and the original GRP scheme [1]. The original GRP scheme was designed for the compressible fluid flows with two related Lagrangian and Eulerian versions. The Eulerian version is always based on the Lagrangian treatment. The transformation is quite delicate, particularly for sonic cases, because it becomes singular at the sonic point. In contrast, our approach leads to a much simpler direct Eulerian scheme. Another approach by the asymptotic analysis can be found in [15, 7]. We mention here the paper [19] where the GRP is solved assuming the solution is given when the initial data have a general analytic distribution on the two sides of cell interface. We note, however, that our solution to the GRP uses only the limiting values of slopes at the interface and thus it is amenable to any given distributions of flow variables adjacent to the cell interface.

The resulting GRP scheme consists of only two steps: (i) the Riemann solver; (ii) the calculation of $(\partial U/\partial t)^n_{j+1/2}$. The (exact or approximate) Riemann solver is standard for many physical systems [18] and references therein. The limiting value $(\partial U/\partial t)^n_{j+1/2}$ is obtained just by solving a linear algebraic system, very close to the linear case (1.8). This linear system can be obtained either by the analytic GRP for (1.1), in which case we label the GRP method as a G_∞–scheme, or by using an acoustic approximation for the GRP, in which case we label the GRP mathod as a G_1-scheme. We note that the G_1-scheme is, in principle, the simplest second order extension of the Godunov scheme, it just adds about $2-5\%$ computation. We mention also that there are a number of intermediate schemes derived from the analytic resolution. In particular, the G_2-scheme is actually equivalent to the MUSCL-scheme, see Appendix D in [1].

For the convenience of the reader, we have structured the paper as follows. Sections 4–6 treat in detail the case of the system consisting of two equations. This enables us to illustrate clearly the role of Riemann invariants and characteristic coordinates. Then in Section 7 we introduce the main topic of the present paper, i.e, the application of the Riemann invariants to general *weakly coupled systems* (WCS). Section 8 is both theoretical and practically important, it introduces an acoustic approximation as the linearized version of nonlinear systems and show how to apply it in the numerical setting. As mentioned above, it leads to a very simple second order extension of the Godunov scheme. Section 9 is devoted to the discussion of the GRP solution in terms of the abstract method developed in the earlier sections. In particular, in Section 9.3 we discuss the system of compressible (non-isentropic) duct flows in the framework of a "weakly coupled system". In Section 10 we give some numerical examples.

2. The setup of GRP scheme

The GRP scheme for the numerical approximation of (1.1) assumes piecewise linear initial data in computational cells and relies on analytical solutions of the generalized Riemann problem at each cell interface. For convenience, we set the cell interface at $x = 0$ and the

initial data as

$$U(x,0)=\begin{cases} U_L+U_L'x, & x<0,\\ U_R+U_R'x, & x>0,\end{cases} \tag{2.1}$$

where U_L, U_R, U_L' and U_R' are constant vectors. We denote by $U(x,t)$ the solution of (1.1) and (2.1). Correspondingly, the limiting values in (1.6) are denoted by

$$U_*=U(0,0_+),\qquad \left(\frac{\partial U}{\partial t}\right)_*=\frac{\partial U}{\partial t}(0,0_+). \tag{2.2}$$

The initial structure of the solution $U(x,t)$ of (1.1) and (2.1) is determined by the associated Riemann problem for

$$\frac{\partial U}{\partial t}+\frac{\partial F(U)}{\partial x}=0,\qquad x\in\mathbb{R},\quad t>0, \tag{2.3}$$

subject to the Riemann initial data

$$U(x,0)=\begin{cases} U_L, & x<0,\\ U_R, & x>0.\end{cases} \tag{2.4}$$

We call the solution of (2.3) and (2.4) the *associated Riemann solution* of (1.1) and (2.1). Our GRP scheme is of the Godunov-type and based on the solvability of (2.3) and (2.4).

Assumption: *The Riemann problem (2.3) and (2.4) is uniquely solvable, thus enabling the Godunov scheme.*

The Riemann solution of (2.3) and (2.4) is self similar and denoted by $R^A(x/t;U_L,U_R)$. Then we have the following proposition [15].

Proposition 2.1. *Let $U(x,t)$ be the solution to the generalized Riemann problem (1.1) and (2.1) and let $R^A(x/t,U_L,U_R)$ be the solution of the associated Riemann problem (2.3) and (2.4). Then for every fixed direction $\lambda=x/t$,*

$$\lim_{t\to 0^+}U(\lambda t,t)=R^A(\lambda;U_L,U_R). \tag{2.5}$$

This implies that the wave configuration for the generalized Riemann problem (1.1) and (2.1) is the same as that for the associated Riemann problem (2.3) and (2.4) near the origin $(x,t)=(0,0)$.

We illustrate this proposition schematically in Figure 2.1. The limiting value U_* in (2.2) (correspondingly $U^n_{j+1/2}$ in (1.6)) is just the Riemann solution along the line $x=0$,

$$U_*=R^A(0;U_L,U_R). \tag{2.6}$$

This is already known and used in the Godunov scheme [9]. They can be obtained with the exact or approximate Riemann solver [18]. Therefore, in order to get the GRP scheme, the main issue is only how to calculate $(\partial U/\partial t)_*$. Once the limiting value $(\partial U/\partial t)_*$ is obtained, we implement the GRP scheme by the following four steps.

Step 1. Given piecewise linear initial data of the type

$$U^n(x)=U^n_j+\sigma^n_j(x-x_j),\quad x\in(x_{j-1/2},x_{j+1/2}), \tag{2.7}$$

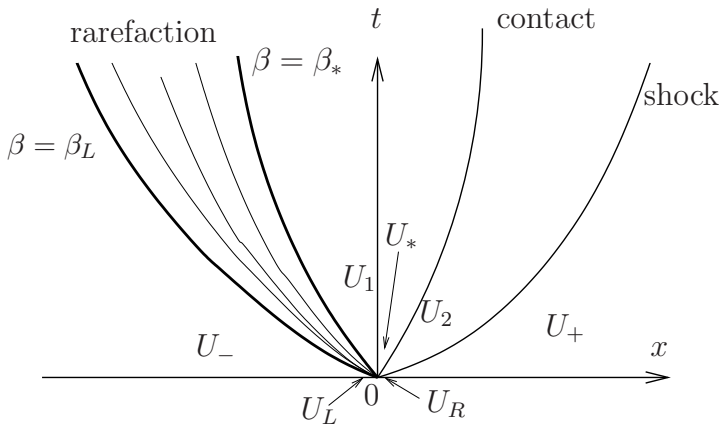

(a) Wave pattern for the GRP

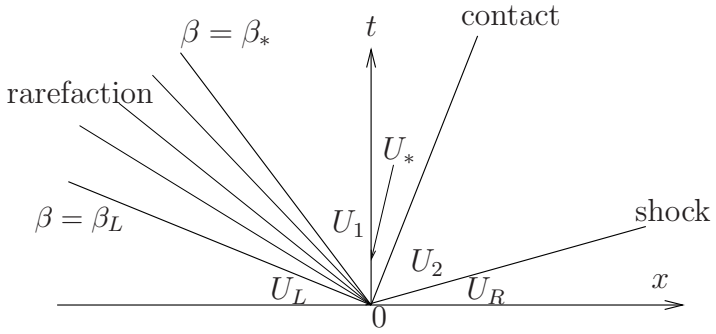

(b) Wave pattern for the associated Riemann problem

FIGURE 2.1. The setup of the GRP scheme

we solve the Riemann problem for (2.3) to define the Riemann solution

$$U^n_{j+1/2} = R^A(0; U^n_j + \frac{\Delta x}{2}\sigma^n_j, U^n_{j+1} - \frac{\Delta x}{2}\sigma^n_{j+1}). \tag{2.8}$$

This is the same as the classical Godunov scheme [9].

Step 2. Determine $(\partial U/\partial t)^n_{j+1/2}$. This is the main theme in the present paper. It turns out that this time derivative of solution vector is obtained by simply solving a linear algebraic system of equations.

Step 3. Approximate numerically the solution of (1.1) by using (1.3) and (1.5).

Step 4. Update the slope by the following procedure. Define

$$\begin{aligned} U^{n+1,-}_{j+1/2} &= U^n_{j+1/2} + \Delta t \left(\frac{\partial U}{\partial t}\right)^n_{j+1/2}, \\ \sigma^{n+1,-}_j &= \frac{1}{\Delta x}(\Delta U)^{n+1,-}_j = \frac{1}{\Delta x}(U^{n+1,-}_{j+1/2} - U^{n+1,-}_{j-1/2}). \end{aligned} \tag{2.9}$$

Then in order to suppress oscillations near discontinuities we modify $\sigma^{n+1,-}_j$ by a monotonicity algorithm to get σ^{n+1}_j, see [1, 12], in the sense of slope limiters. For the numerical

examples in Section 10, we use the following limiter

$$\sigma_j^{n+1} = \text{minmod}\left(\alpha\frac{U_j^{n+1}-U_{j-1}^{n+1}}{\Delta x}, \sigma_j^{n+1,-}, \alpha\frac{U_{j+1}^{n+1}-U_j^{n+1}}{\Delta x}\right), \tag{2.10}$$

where the parameter $\alpha \in [0, 2)$.

Remark 2.2. In comparison with other (even first order) upwind schemes, we at most need to solve a linear system of algebraic equations additionally. For the G_1-scheme to be presented in Section 8, we need to solve a linear system of algebraic equations exactly. Compared with the Godunov scheme, just additional $2 \sim 5\%$ of computation time is required in most practical cases.

3. Heuristic explanation from a linear system

In this section we use a familiar linear system to explain the necessity to introduce the Riemann invariants in upwind (the Godunov-type) schemes. The linear example is

$$\frac{\partial u}{\partial t} + c\frac{\partial v}{\partial x} = 0, \qquad \frac{\partial v}{\partial t} + c\frac{\partial u}{\partial x} = 0, \tag{3.1}$$

where $c > 0$ is constant. This model describes two linear waves: One propagates to the left with velocity $-c$ and the other to the right with velocity c.

For the given initial data of type (2.1), where $U = (u, v)^\top$, the solution is discontinuous at the origin and the discontinuities propagate along characteristics. Therefore we are not able to use (3.1) to simply get $\partial u/\partial t$ and $\partial v/\partial t$, as in the single equation case. However, if (3.1) is written in the following form

$$\frac{\partial(u-v)}{\partial t} - c\frac{\partial(u-v)}{\partial x} = 0, \qquad \frac{\partial(u+v)}{\partial t} + c\frac{\partial(u+v)}{\partial x} = 0, \tag{3.2}$$

we see that the function $u + v$ (resp. $u - v$) is smooth on the two sides of the characteristic $dx/dt = c$ (resp. $dx/dt = -c$). The functions $u \pm v$ correspond to the Riemann invariants in nonlinear cases. Turning back to the system (3.1), we denote $u'_* = \lim\limits_{t\to 0^+}(\partial u/\partial x)(0, t)$ (similarly for v'_*). Then we can proceed, as in scalar cases, to get

$$\begin{aligned} &u_* + v_* = u_L + v_L, \qquad u'_* + v'_* = u'_L + v'_L, \\ &u_* - v_* = u_R - v_R, \qquad u'_* - v'_* = u'_R - v'_R. \end{aligned} \tag{3.3}$$

By using (3.2), we have

$$\left(\frac{\partial u}{\partial t}\right)_* + \left(\frac{\partial v}{\partial t}\right)_* = -c(u'_L + v'_L), \quad \left(\frac{\partial u}{\partial t}\right)_* - \left(\frac{\partial v}{\partial t}\right)_* = c(u'_R - v'_R). \tag{3.4}$$

In order to get $(\partial u/\partial t)_*$ and $(\partial v/\partial t)_*$, we need to solve (3.4) and get

$$\left(\frac{\partial u}{\partial t}\right)_* = -\frac{c(u'_L + v'_L)}{2} + \frac{c(u'_R - v'_R)}{2}, \quad \left(\frac{\partial v}{\partial t}\right)_* = -\frac{c(u'_L + v'_L)}{2} - \frac{c(u'_R - v'_R)}{2}. \tag{3.5}$$

This is essentially the solution of GRP for (3.1).

We summarize the above process in the following two steps:

(i) Find Riemann invariants and obtain their time derivatives. Thus the system of linear equations (3.4) is derived.

(ii) Solve the resulting linear system of algebraic equations to yield the limiting values $(\partial u/\partial t)_*$ and $(\partial v/\partial t)_*$.

In the nonlinear case of (1.1), we also perform these two steps. In particular, the concept of Riemann invariants plays a pivotal role and corresponds to the quantities $u+v$ and $u-v$ here. They are used to analytically resolve the rarefaction waves in the generalized Riemann problem (1.1) and (2.1), which constitutes the important feature of the resulting scheme. In addition, they are useful in resolving contact discontinuities.

4. The resolution of rarefaction waves in the two-equation system

In this section we focus on the case of a strictly hyperbolic system of two equations. We note that the physical models of isentropic (compressible) flows and shallow water equations are examples of such systems. Furthermore, we shall later show that the main idea here carries over to a broader class of general systems.

Thus, we assume that (1.1) consists of two equations and denote $U = (u, v)^\top$ and $F = (f(u, v), g(u, v))^\top$. The Jacobian matrix $DF(U) = \partial F/\partial U$ has two distinct eigenvalues

$$\lambda(u, v) < \mu(u, v), \tag{4.1}$$

and further assume that λ is genuinely nonlinear, and thus its associated wave is either a rarefaction wave or a shock [8]. As in [8, Sec. 7.3] the system is endowed with a coordinate system of Riemann invariants which we shall denote by ϕ and ψ. In terms of these new unknowns (1.1) is reduced into the form

$$\begin{cases} \dfrac{\partial \phi}{\partial t} + \lambda(\phi, \psi)\dfrac{\partial \phi}{\partial x} = k_1(x, \phi, \psi), \\ \\ \dfrac{\partial \psi}{\partial t} + \mu(\phi, \psi)\dfrac{\partial \psi}{\partial x} = k_2(x, \phi, \psi), \end{cases} \tag{4.2}$$

where k_1 and k_2 are two functions resulting from the source term of (1.1) and they are expressed in terms of the Riemann invariants ϕ, ψ. For uniformity, we denote $W = (\phi, \psi)^\top$, $K = (k_1, k_2)^\top$ and $\Lambda = \mathrm{diag}(\lambda, \mu)$. Then (4.2) is rewritten as

$$\frac{\partial W}{\partial t} + \Lambda(W)\frac{\partial W}{\partial x} = K(x, W). \tag{4.3}$$

As pointed out earlier, the main feature of the GRP scheme is the resolution of rarefaction waves. In this context, it will turn out that the concept of characteristic coordinates is quite useful.

4.1. **Characteristic coordinates.**

The characteristic coordinates, as the integral curves of characteristic equations, play an important role in the resolution of rarefaction waves and simplify the calculation. Let $C^\lambda : \beta(x, t) = const.$ be the integral curve of the differential equation

$$\frac{dx}{dt} = \lambda(\phi, \psi), \tag{4.4}$$

and $C^\mu : \alpha(x,t) = const.$ be the integral curve of the differential equation

$$\frac{dx}{dt} = \mu(\phi, \psi). \tag{4.5}$$

Consider a domain in the (x,t)-plane where the coordinates (x,t) can be obtained as functions of α and β. This transformation is denoted by

$$t = t(\alpha, \beta), \qquad x = x(\alpha, \beta). \tag{4.6}$$

In terms of the characteristic coordinates (α, β), the system (4.2) can be rewritten in the form of the characteristic equations

$$\begin{cases} \dfrac{\partial x}{\partial \alpha} = \lambda(\phi,\psi)\dfrac{\partial t}{\partial \alpha}, \qquad \dfrac{\partial \phi}{\partial \alpha} = \dfrac{\partial t}{\partial \alpha} \cdot k_1(x(\alpha,\beta),\phi,\psi), \\ \\ \dfrac{\partial x}{\partial \beta} = \mu(\phi,\psi)\dfrac{\partial t}{\partial \beta}, \qquad \dfrac{\partial \psi}{\partial \beta} = \dfrac{\partial t}{\partial \beta} \cdot k_2(x(\alpha,\beta),\phi,\psi). \end{cases} \tag{4.7}$$

It follows, by differentiating the first pair of equations with respect to β, the second with respect to α and subtracting, that $t = t(\alpha, \beta)$ satisfies,

$$(\lambda - \mu)\frac{\partial^2 t}{\partial \alpha \partial \beta} + \frac{\partial \lambda}{\partial \beta}\frac{\partial t}{\partial \alpha} - \frac{\partial \mu}{\partial \alpha}\frac{\partial t}{\partial \beta} = 0. \tag{4.8}$$

We differentiate the ψ-equation in (4.7) with respect to α and incorporate (4.8) into the resulting equation to get that $\psi = \psi(\alpha, \beta)$ satisfies

$$\begin{aligned} \frac{\partial^2 \psi}{\partial \alpha \partial \beta} &= \frac{\partial^2 t}{\partial \alpha \partial \beta} \cdot k_2(x(\alpha,\beta),\phi,\psi) + \frac{\partial t}{\partial \beta}\frac{\partial k_2}{\partial \alpha} \\ &= -\frac{k_2}{\lambda - \mu} \cdot \frac{\partial \lambda}{\partial \beta} \cdot \frac{\partial t}{\partial \alpha} + \frac{\partial t}{\partial \beta}\left(\frac{k_2}{\lambda - \mu}\frac{\partial \mu}{\partial \alpha} + \frac{\partial k_2}{\partial \alpha}\right). \end{aligned} \tag{4.9}$$

Similarly, we have the second order equation for the Riemann invariant ϕ,

$$\frac{\partial^2 \phi}{\partial \alpha \partial \beta} = -\frac{k_1}{\mu - \lambda} \cdot \frac{\partial \mu}{\partial \alpha} \cdot \frac{\partial t}{\partial \beta} + \frac{\partial t}{\partial \alpha}\left(\frac{k_1}{\mu - \lambda}\frac{\partial \lambda}{\partial \beta} + \frac{\partial k_1}{\partial \beta}\right). \tag{4.10}$$

Next we turn to the detailed analysis of the rarefaction wave for the generalized Riemann problem (1.1) and (2.1). In view of Proposition 2.1, when approaching the origin $(x,t) = (0,0)$, the solution $U(x,t)$ is determined by the associated Riemann solution $R^A(x/t; U_L, U_R)$. We can therefore regard the former as a perturbation of the latter. When investigating the (curved) centered rarefaction wave for the generalized Riemann problem, we will use the same domain of characteristic coordinates as the one determined by the associated rarefaction wave.

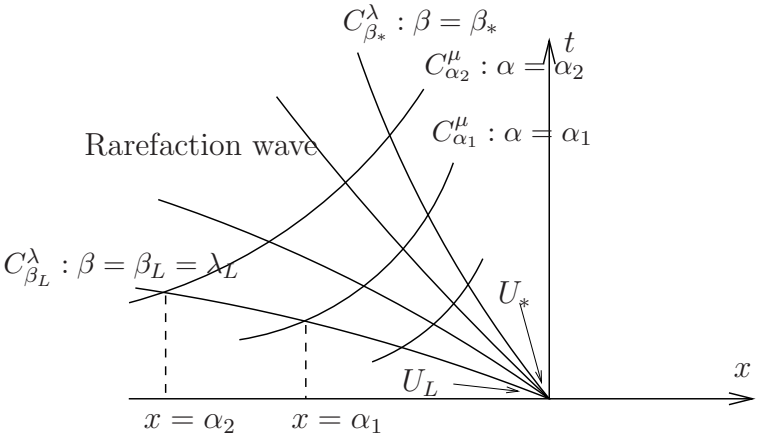

(a) The curved rarefaction wave in the generalized Riemann problem

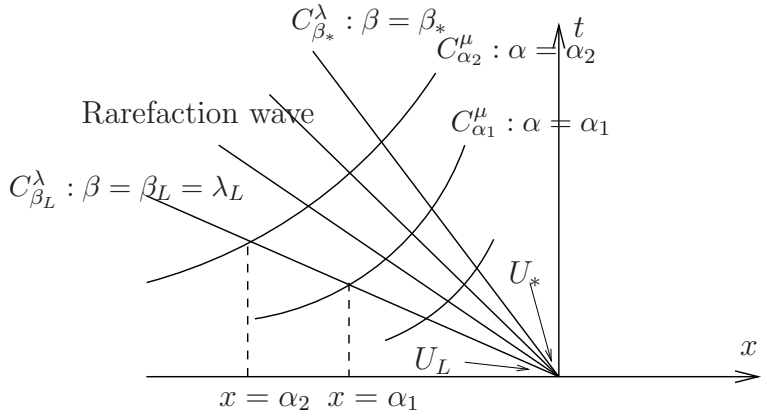

(b) The rarefaction wave in the associated Riemann problem

FIGURE 4.1. Characteristic coordinates throughout a centered rarefaction wave

4.2. **The resolution of rarefaction waves.** We start with the associated rarefaction wave for the Riemann problem (2.3) and (2.4). We assume the structure as in Figure (4.1)(b) and the rarefaction wave is denoted by R^A_λ. Further, the $t-$axis is located in the smooth domain behind the rarefaction wave R^A_λ.

Since ψ is constant across the rarefaction wave R^A_λ, we express it by using

$$\begin{cases} \lambda(\phi, \psi) = x/t, \\ \psi = \psi_L, \end{cases} \tag{4.11}$$

where ψ_L is the value of ψ at the head characteristic of R^A_λ, i.e. $\beta = \beta_L$. This rarefaction wave expands from β_L up to β_*. We define the characteristic coordinate $\beta = x/t$. The characteristic coordinate α is defined as follows. In view of (4.11), one has $\lambda(\phi, \psi_L) = \beta$, which can be inverted to yield,

$$\phi = \phi(x/t; \psi_L) = \phi(\beta; \psi_L). \tag{4.12}$$

Then the characteristic curve $C^{\mu}_{\alpha_0} : \alpha(x,t) = \alpha_0$ is defined to be the integral curve of the equation

$$\frac{dx}{dt} = \mu(\phi,\psi) = \mu(\phi(x/t;\psi_L),\psi_L), \tag{4.13}$$

where the constant α_0 is chosen to be the x-coordinate of the intersection point of $C^{\mu}_{\alpha_0}$ with the leading λ-characteristic curve $C^{\lambda}_{\beta_L}$. This determines (x,t) as functions of (α,β).

Denote the corresponding characteristic map to the (x,t)-plane by

$$t = t_{ass}(\alpha,\beta), \quad x = x_{ass}(\alpha,\beta). \tag{4.14}$$

All other variables including the eigenvalues λ, μ and Riemann invariants can now be expressed as smooth functions of (α,β). We observe that the characteristic map is singular at $\alpha = 0$, where the segment between β_L and β_* is mapped to the origin $(x,t) = (0,0)$. We note that $t_{ass}(\alpha,\beta)$ satisfies at $\alpha = 0$, in view of (4.8) and the fact that $(\partial t_{ass}/\partial\beta)(0,\beta) = 0$, that

$$(\lambda-\mu)\frac{\partial^2 t_{ass}}{\partial\alpha\partial\beta}(0,\beta) = -\frac{\partial t_{ass}}{\partial\alpha}(0,\beta)\cdot\frac{\partial\lambda}{\partial\beta}(0,\beta). \tag{4.15}$$

Since $(\partial\lambda/\partial\beta)(0,\beta) = 1$, by the definition of β-coordinate, we get

$$\frac{\partial t_{ass}}{\partial\alpha}(0,\beta) = \frac{\partial t_{ass}}{\partial\alpha}(0,\beta_L)\exp\left(\int_{\beta_L}^{\beta}\frac{1}{(\mu-\lambda)(0,\xi)}d\xi\right). \tag{4.16}$$

By our choice of the α-coordinate as the x-value of the intersection point of C^{μ}_{α} with the leading characteristic $C^{\lambda}_{\beta_L}$, we obtain $(\partial x_{ass}/\partial\alpha)(0,\beta_L) = 1$. Then we use (4.7) to get

$$\frac{\partial t_{ass}}{\partial\alpha}(0,\beta_L) = \frac{1}{\beta_L}\frac{\partial x_{ass}}{\partial\alpha}(0,\beta_L) = \frac{1}{\beta_L}. \tag{4.17}$$

This together with (4.16) gives the explicit expressions for the derivatives of $t_{ass}(\alpha,\beta)$, $x_{ass}(\alpha,\beta)$ at the singularity point $(x,t) = (0,0)$,

$$\begin{aligned}
&\frac{\partial t_{ass}}{\partial\alpha}(0,\beta) = \frac{1}{\beta_L}\exp\left(\int_{\beta_L}^{\beta}\frac{1}{\mu(0,\xi)-\xi}d\xi\right),\\
&\frac{\partial x_{ass}}{\partial\alpha}(0,\beta) = \frac{\beta}{\beta_L}\exp\left(\int_{\beta_L}^{\beta}\frac{1}{\mu(0,\xi)-\xi}d\xi\right).
\end{aligned} \tag{4.18}$$

Remark 4.1. Inspecting (4.11), (4.12) and (4.16), we see that the ratio between $(\partial t_{ass}/\partial\alpha)(0,\beta)$ and $(\partial t_{ass}/\partial\alpha)(0,\beta_L)$ is function of β and is independent of the α-coordinate. Therefore, we retain the degree of freedom in our choice of α, which will simplify some calculation, see Section 9.

In the following we turn to deal with the generalized Riemann problem (1.1) and (2.1), and consider the general (curved) rarefaction wave, see Figure 4.1(a). The characteristic curves inside the curved rarefaction wave $t = t(\alpha,\beta)$, $x = x(\alpha,\beta)$ are second order approximations of $t_{ass}(\alpha,\beta)$ and $x_{ass}(\alpha,\beta)$ as $\alpha\to 0$. This fact is stated in the following proposition and the proof is omitted in the present paper.

Proposition 4.2. *As $\alpha \to 0$, we have the following asymptotic expressions for $t(\alpha,\beta)$, $x(\alpha,\beta)$,*

$$t(\alpha,\beta) = t_{ass}(\alpha,\beta) + O(\alpha^2), \quad x(\alpha,\beta) = x_{ass}(\alpha,\beta) + O(\alpha^2), \tag{4.19}$$

where $\beta_L \le \beta \le \beta_*$.

With this proposition, we have the following theorems about the resolution of the rarefaction wave.

Theorem 4.3. *Let $\psi_\alpha(0,\beta) = \frac{\partial\psi}{\partial\alpha}(0,\beta)$. Then throughout the rarefaction wave associated with λ, we have*

$$\psi_\alpha(0,\beta) = \psi_\alpha(0,\beta_L) + \int_{\beta_L}^{\beta} -\frac{k_2}{\lambda-\mu}(0,\xi)\cdot\frac{\partial t_{ass}}{\partial\alpha}(0,\xi)d\xi, \quad \beta_L \le \beta \le \beta_*. \tag{4.20}$$

The initial datum $\psi_\alpha(0,\beta_L)$ is

$$\psi_\alpha(0,\beta_L) = \psi'_L + \frac{1}{\beta_L}(k_{2,L} - \mu_L\psi'_L), \tag{4.21}$$

where ψ'_L is determined by U_L, U'_L as in (2.1) and $k_{2,L} = k_2(0,\phi_L,\psi_L)$ (see the RHS of (4.2)).

Proof. Recall that

$$\frac{\partial t(0,\beta)}{\partial\beta} = 0, \quad \frac{\partial x(0,\beta)}{\partial\beta} = 0. \tag{4.22}$$

The asymptotic behavior of solutions at the origin, see Proposition 4.2, shows

$$\frac{\partial t}{\partial\alpha}(0,\beta) = \frac{\partial t_{ass}}{\partial\alpha}(0,\beta), \quad \frac{\partial x}{\partial\alpha}(0,\beta) = \frac{\partial x_{ass}}{\partial\alpha}(0,\beta). \tag{4.23}$$

Therefore, setting $\alpha = 0$ in (4.9), we obtain

$$\frac{\partial}{\partial\beta}\left(\psi_\alpha(0,\beta)\right) = -\frac{k_2}{\lambda-\mu}(0,\beta)\cdot\frac{\partial t_{ass}}{\partial\alpha}(0,\beta), \quad \beta\in(\beta_L,\beta_*), \tag{4.24}$$

which yields (4.20) by integration.

The initial datum $\psi_\alpha(0,\beta_L)$ comes from the characteristic form (4.7) by using the chain rule,

$$\begin{aligned}\frac{\partial\psi}{\partial\alpha}(0,\beta_L) &= \frac{\partial\psi}{\partial x}(0,\beta_L)\frac{\partial x}{\partial\alpha}(0,\beta_L) + \frac{\partial\psi}{\partial t}(0,\beta_L)\frac{\partial t}{\partial\alpha}(0,\beta_L)\\ &= \psi'_L + \frac{\partial\psi}{\partial t}(0,\beta_L)\cdot\frac{1}{\beta_L},\end{aligned} \tag{4.25}$$

where we use the fact that $(\partial x/\partial\alpha)(0,\beta_L) = 1$ and $(\partial t/\partial\alpha)(0,\beta_L) = 1/\beta_L$. Then we use the ψ-equation in (4.2) to get (4.21). □

Theorem 4.4. *Consider the rarefaction wave R_λ associated with λ. Then we have*

$$a_L\left(\frac{\partial u}{\partial t}\right)_* + b_L\left(\frac{\partial v}{\partial t}\right)_* = d_L^*, \tag{4.26}$$

where $(a_L, b_L) = (\nabla_U \psi)_*$, $\nabla_U \psi = (\partial\psi/\partial u, \partial\psi/\partial v)$ *and*

$$d_L^* = \frac{\mu_*}{\mu_* - \lambda_*} \cdot \left(\psi_\alpha(0, \beta_*) \cdot \left(\frac{\partial t_{ass}}{\partial \alpha} \right)^{-1} (0, \beta_*) - \frac{\lambda_*}{\mu_*} \cdot k_2(0, \phi_*, \psi_*) \right). \tag{4.27}$$

Proof. We use the result of Theorem 4.3 at $\beta = \beta_*$ and express the directional derivative in terms of (x, t) derivatives. Using the equations for ψ in (4.7) and (4.2), one obtains,

$$\begin{aligned} \psi_\alpha(0, \beta_*) = & \frac{\partial t_{ass}(0, \beta_*)}{\partial \alpha} \cdot \left(\frac{\partial \psi}{\partial t} + \lambda \frac{\partial \psi}{\partial x} \right) (0, \beta_*) \\ & = \frac{\partial t_{ass}(0, \beta_*)}{\partial \alpha} \left[\left(\frac{\partial \psi}{\partial t} \right)_* + \frac{\lambda_*}{\mu_*} \left(- \left(\frac{\partial \psi}{\partial t} \right)_* + k_2(0, \phi_*, \psi_*) \right) \right]. \end{aligned} \tag{4.28}$$

It follows that,

$$\left(\frac{\partial \psi}{\partial t} \right)_* = \frac{\mu_*}{\mu_* - \lambda_*} \cdot \left[\psi_\alpha(0, \beta_*) \cdot \left(\frac{\partial t_{ass}}{\partial \alpha} \right)^{-1} (0, \beta_*) - \frac{\lambda_*}{\mu_*} \cdot k_2(0, \phi_*, \psi_*) \right], \tag{4.29}$$

where $\lambda_* = \beta_*$. We note that ψ is regular across the characteristic $C^\lambda_{\beta_*}$. Hence the value of $\psi_\alpha(0, \beta_*)$ can be evaluated using the values of $\partial\psi/\partial t$, $\partial\psi/\partial x$ in the smooth domain behind the rarefaction wave R_λ. We write ψ in terms of U and immediately arrive at (4.26). □

Remark 4.5. Note that the term $\psi_\alpha(0, \beta_*) \cdot \left(\frac{\partial t_{ass}}{\partial \alpha} \right)^{-1} (0, \beta_*)$ is clearly independent of the choice of α, cf. Remark 4.1.

Remark 4.6. Since ψ is constant throughout R^A_λ in the associated Riemann solution, ψ is still regular even when the initial data has non-zero slopes and the source term is present in the governing equation (4.2). This is the reason that we can resolve the rarefaction wave in terms of ψ. Note that $\phi_\alpha(0, \beta_*) = k_1(0, \phi_*, \psi_*) \cdot (\partial t_{ass}/\partial \alpha)(0, \beta_*)$. Hence we cannot use it to get $(\partial\phi/\partial t)_*$, and thus this relation cannot be used to obtain $(\partial U/\partial t)_*$.

5. The resolution of shocks for the two-equation system

In this section we continue the investigation of the two-equation system (as in Section 4) by discussing the resolution of shocks. We assume that the wave associated with the μ family is a shock moving to the right and let the shock trajectory be $x = x(t)$ with the speed $\sigma(t) = x'(t)$, separating two limiting states U, $\overline{U}$. To fix the ideas, we assume that $\overline{U}$ is the state ahead of the shock while U is the state behind it. This shock is described by the Rankine-Hugoniot jump condition,

$$F(U) - F(\overline{U}) = \sigma(U - \overline{U}). \tag{5.1}$$

Then we know [8, Section 8.2] that if a state U connects to $\overline{U}$ by the shock with speed σ, (5.1) gives the Hugoniot locus of the form,

$$\begin{cases} \sigma = \sigma(U, \overline{U}), \\ U = \overline{U} + \tau K(U, \overline{U}), \end{cases} \tag{5.2}$$

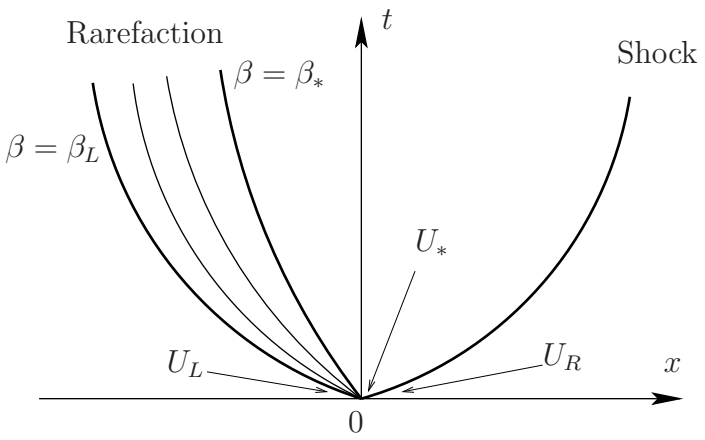

FIGURE 5.1. A typical wave pattern for the two-equation case

where $\tau > 0$ is a parameter describing the strength of the shock. In fact, the system (5.2) corresponds to one of the two shock curves associated with λ, μ (recall that λ, μ are two genuinely nonlinear eigenvalues for the system of two equations in Section 4). Eliminating the parameter τ from (5.2) yields a single equation connecting the state $\overline{U} = (\overline{u}, \overline{v})$ to the state $U = (u, v)$, given by

$$\Psi(U; \overline{U}) = 0. \tag{5.3}$$

This is indeed the equation for the Hugoniot curve in the state (u, v)-plane, and it holds along the shock trajectory $x = x(t)$ identically. Note that U, $\overline{U}$ are the limiting states on both sides of $x = x(t)$, $U = U(x(t), t)$, $\overline{U} = \overline{U}(x(t), t)$, where we are now using U and $\overline{U}$ also for the full states behind and ahead of the shock, respectively.

In terms of Riemann invariants W (see (4.3) for the notation W), we can rewrite (5.3) in the form

$$\Phi(W; \overline{W}) = 0. \tag{5.4}$$

We may therefore differentiate (5.4) in the direction of the shock $x = x(t)$ and get

$$\nabla_W \Phi \cdot \left(\frac{\partial W}{\partial t} + \sigma \frac{\partial W}{\partial x} \right) = -\nabla_{\overline{W}} \Phi \cdot \left(\frac{\partial \overline{W}}{\partial t} + \sigma \frac{\partial \overline{W}}{\partial x} \right). \tag{5.5}$$

We want to solve (5.5) for $\partial W/\partial t$. We are assuming that the t-axis is located in the intermediate region so that $\lambda < 0$ and $\mu > 0$ (see Figure 5.1). In the sonic case where the t-axis is located in the rarefaction wave, we already have the full solution, see Subsection 6.1 below. We use the diagonal form (4.3) to obtain,

$$\frac{\partial W}{\partial x} = \Lambda(W)^{-1} \left(-\frac{\partial W}{\partial t} + K(x, W) \right), \qquad \frac{\partial \overline{W}}{\partial t} = -\Lambda(\overline{W}) \frac{\partial \overline{W}}{\partial x} + K(x, \overline{W}). \tag{5.6}$$

Note that the limiting values of σ, W, $\overline{W}$, $\partial W/\partial t$ and $\partial \overline{W}/\partial x$ (see Eqs. (2.1), (2.2)) are

(5.7)

$$\lim_{t \to 0^+} \sigma = \sigma_0, \quad \lim_{t \to 0^+} W = W_*, \quad \lim_{t \to 0^+} \frac{\partial W}{\partial t} = \left(\frac{\partial W}{\partial t} \right)_*, \quad \lim_{t \to 0^+} \overline{W} = W_R, \quad \lim_{t \to 0^+} \frac{\partial \overline{W}}{\partial x} = W_R',$$

where the limits in (5.7) correspond to our assumption that $\sigma_0 > 0$, so that the shock moves into the domain $x > 0$, leaving the t-axis in the smooth domain behind it. It is clear how to change the limits when $\sigma_0 < 0$. Then we use (5.6), (5.7) in (5.5) so as to obtain

(5.8)
$$\nabla_W \Phi(W_*; W_R)(I - \sigma_0 \Lambda(W_*)^{-1}) \left(\frac{\partial W}{\partial t}\right)_*$$
$$= -\sigma_0 \nabla_W \Phi(W_*; W_R)\Lambda(W_*)^{-1} K(0, W_*) - \nabla_{\overline{W}} \Phi(W_*; W_R) \left[(\sigma_0 I - \Lambda(W_R))W_R' + K(0, W_R)\right].$$

We express $\partial W/\partial t$ in terms of $\partial U/\partial t$ (as in the end of the proof of Theorem 4.4), in order to obtain the following theorem.

Theorem 5.1. *Consider the two equation system (1.1) , subject to the initial data (2.1). Assume that the wave pattern is as in Figure 5.1, i.e., the wave associated with the μ family is a shock moving to the right and that the t-axis is contained in the smooth region behind it. Then the two components of $(\partial U/\partial t)_*$ (see (2.2)) satisfy the following linear equation at the singularity $(x, t) = (0, 0)$,*

$$a_R \left(\frac{\partial u}{\partial t}\right)_* + b_R \left(\frac{\partial v}{\partial t}\right)_* = d_R, \tag{5.9}$$

where the coefficients a_R, b_R and d_R are given explicitly as

$$\begin{aligned} (a_R, b_R) = \;& \nabla_W \Phi(W_*; W_R)(I - \sigma_0 \Lambda(W_*)^{-1}) DW(U_*), \\ d_R = \;& -\sigma_0 \nabla_W \Phi(W_*; W_R)\Lambda(W_*)^{-1} K(0, W_*) \\ & -\nabla_{\overline{W}} \Phi(W_*; W_R) \left[(\sigma_0 I - \Lambda(U_R))W_R' + K(0, W_R)\right]. \end{aligned} \tag{5.10}$$

Remark 5.2. If the eigenvalue μ is linearly degenerate, the corresponding jump discontinuity is a contact discontinuity. For this case, $\sigma(W, \overline{W}) = \mu(W) = \mu(\overline{W})$ and in the limit

$$I - \sigma_0 \Lambda(W_*)^{-1} = \begin{pmatrix} (\lambda_* - \mu_*)/\lambda_* & 0 \\ 0 & 0 \end{pmatrix}, \qquad \sigma_0 I - \Lambda(W_R) = \begin{pmatrix} \mu_R - \lambda_R & 0 \\ 0 & 0 \end{pmatrix}, \tag{5.11}$$

The first component of equation (5.8) gives a scalar equation

(5.12)
$$\frac{\partial \Phi(W_*; W_R)}{\partial \phi} \cdot \frac{\lambda_* - \mu_*}{\lambda_*} \cdot \left(\frac{\partial \phi}{\partial t}\right)_*$$
$$= -\mu_* \nabla_W \Phi(W_*; W_R)\Lambda(W_*)^{-1} K(0, W_*) - \frac{\partial \Phi(W_*; W_R)}{\partial \phi} \cdot (\mu_R - \lambda_R) \cdot (\phi_R' + k_1(0, W_R)).$$

These arguments also apply to the acoustic case that will be discussed later on. The idea will be used to consider weak shocks as characteristic curves, thus treating the weak shocks as linearly degenerate discontinuities. Clearly we can also obtain a linear equation in the

same form as (5.9) with coefficients

(5.13)

$$(a_R, b_R) = \frac{\partial \Phi(W_*; W_R)}{\partial \phi} \cdot \frac{\lambda_* - \mu_*}{\lambda_*} \cdot (\nabla_U \phi)_*,$$

$$d_R = -\mu_* \nabla_W \Phi(W_*; W_R) \Lambda(W_*)^{-1} K(0, W_*) - \frac{\partial \Phi(W_*; W_R)}{\partial \phi} \cdot (\mu_R - \lambda_R) \cdot (\phi'_R + k_1(0, W_R)).$$

6. The time derivative of solutions at the singularity for the two-equation system

In this section we summarize the results of Sections 4 and 5 in order to present the full solution to the generalized Riemann problem for (1.1) in the two equation case, subject to the initial condition (2.1) at the singularity. As has already been mentioned in the Introduction, this case represents significant physical models. In addition, we shall see in the following section how this solution can be readily extended to many important cases of larger systems of conservation laws.

Theorem 6.1. *Assume that the local wave pattern for the generalized Riemann problem (1.1) is as depicted in Figure 5.1, and the t-axis is inside the intermediate (smooth) region. Then the limiting value $(\partial U/\partial t)_*$ can be obtained by solving the following pair of linear algebraic equations,*

$$\begin{cases} a_L \left(\dfrac{\partial u}{\partial t}\right)_* + b_L \left(\dfrac{\partial v}{\partial t}\right)_* = d_L, \\ \\ a_R \left(\dfrac{\partial u}{\partial t}\right)_* + b_R \left(\dfrac{\partial v}{\partial t}\right)_* = d_R, \end{cases} \tag{6.1}$$

where a_L, b_L and d_L are given in Theorem 4.4 and a_R, b_R and d_R are given in Theorem 5.1.

6.1. **The sonic case.** Special attention should be paid to the case where the t-axis (the cell interface $x = 0$) is contained in the rarefaction wave, so that it is tangential to one of The characteristic curves. We refer to this case as a *sonic case.* Then we have to modify the above approach. Indeed, it becomes much simpler. We still use the notations in Section 4. Consider the rarefaction wave associated with λ. We see that the equation (4.26) for ψ is still valid, where β_* is replaced by $\beta_0 = 0$. In addition, let $C^{\lambda}_{\beta_0}$ be the characteristic curve tangent to the t-axis, $\beta_L < \beta_0 = 0 < \beta_*$, so that we have $\lambda(\phi_0, \psi_0) = 0$. Then we obtain from (4.7), with $\beta_* = \beta_0$,

$$\phi_\alpha(0, \beta_*) = k_1(0, \phi_*, \psi_*) \cdot (\partial t_{ass}/\partial \alpha)(0, \beta_*) \tag{6.2}$$

That is,

$$(\nabla_U \phi)_0 \left(\frac{\partial U}{\partial t}\right)_* = k_1(0, \phi_0, \psi_0). \tag{6.3}$$

We therefore obtain in this case the following theorem.

Theorem 6.2. *(Sonic case). Assume that the t-axis is located inside the rarefaction wave associated with λ. Then we can calculate the limiting values of the time derivatives $(\partial U/\partial t)_*$*

by solving the following system of two linear algebraic equations,

$$(\nabla_U \psi)_0 \left(\frac{\partial U}{\partial t}\right)_* = d_L^0,$$

$$(\nabla_U \phi)_0 \left(\frac{\partial U}{\partial t}\right)_* = k_1(0, \phi_0, \psi_0), \tag{6.4}$$

where d_L^0 is defined in (4.27), $d_L^0 = \psi_\alpha(0,0) \cdot (\partial t_{ass}/\partial\alpha)^{-1}(0,0)$ (see Eq. (4.18) with $\beta = 0$ for $(\partial t_{ass}/\partial\alpha)(0,\beta)$).

7. The resolution of the generalized Riemann problem for weakly coupled systems

In this section we extend the methodology in the previous sections in order to investigate the general hyperbolic system with three or more equations ($m \geq 3$). As is well-known, the system (1.1) is in general not endowed with a coordinate system of Riemann invariants and hence it cannot be reduced to a diagonal characteristic form analogous to (4.2) for the system of two equations. However, for many physical systems that are called *weakly coupled systems*(WCS) in the present paper, we are still able to use the concept of Riemann invariants in order to resolve rarefaction waves in the generalized Riemann problem. Such systems include the compressible fluid flows, the example of electrophoresis etc [8, Page 130].

Also we can extend the method of Section 5 in order to resolve jump discontinuities, shocks and contact discontinuities. Note that the concept of Riemann invariants simplifies the resolution of contact discontinuities.

We assume the Jacobian matrix $DF = \partial F/\partial U$ has a complete set of right eigenvectors $\Upsilon_i(U)$

$$DF(U)\Upsilon_i(U) = \lambda_i \Upsilon_i(U), \tag{7.1}$$

where λ_i, $i = 1, \cdots, m$, are the eigenvalues of DF and ordered as

$$\lambda_1 < \lambda_2 < \cdots < \lambda_m. \tag{7.2}$$

In this section, we assume that the rarefaction wave associated with λ_i moves to the left and the jump discontinuity associated with λ_i moves to the right. We further suppose that the limiting values $(\partial U/\partial x)_l$ of spatial derivatives on the left-hand side of the rarefaction wave, and the limiting values $(\partial U/\partial x)_r$ on the right-hand side of the jump discontinuity, respectively, are known. The modification needed in other cases will be obvious.

7.1. **The resolution of rarefaction waves.** Since the local structure of the solution of (1.1) and (2.1) is determined by the associated Riemann solution of the corresponding homogeneous hyperbolic conservation laws, we first take a look at the homogeneous case (2.3). An i-Riemann invariant of (2.3) is a smooth scalar function E such that

$$DE(U)\Upsilon_i(U) = 0, \quad DE(U) = \left(\frac{\partial E}{\partial u_1}, \cdots, \frac{\partial E}{\partial u_m}\right). \tag{7.3}$$

The system (2.3) is endowed with a coordinate system of Riemann invariants if there exist functions $w_1, \cdots, w_m$, such that for any $i, j = 1, \cdots, m$ with $i \neq j$, w_j is an i-Riemann

invariant of (2.3), and for every $1 \le i \le m$, $Dw_i(U)\Upsilon_i(U) \neq 0$. With these Riemann invariants, (2.3) is reduced into a diagonal system

$$\frac{\partial w_i}{\partial t} + \lambda_i(W)\frac{\partial w_i}{\partial x} = 0, \quad W = (w_1, \cdots, w_m)^\top, \quad i = 1, \cdots, m. \tag{7.4}$$

We refer to [8, Section 7.3] for details.

Fix the index i and assume that λ_i is genuinely nonlinear,

$$\nabla\lambda_i \cdot \Upsilon_i = 1, \quad i = 1, \cdots, m. \tag{7.5}$$

Consider the corresponding rarefaction wave R_i^A, which is a part of the solution of the associated Riemann problem (2.3) subject to the initial data (2.4). We represent it by $U^A(x,t) = V(x/t)$, $i = 1, \cdots, m$, where

$$\lambda_i(V(\xi)) = \xi, \quad \frac{dV}{d\xi} = \Upsilon_i(V(\xi)), \quad \xi = x/t. \tag{7.6}$$

Now we use the vector W of Riemann invariants as the state vector. In particular, the functions depending on U can be expressed in terms of W without changing their notations. The i-Riemann invariants, w_j, $j \neq i$, are constant, $w_j \equiv A_j$, across the rarefaction wave R_i^A so that this rarefaction wave is expressed by using

$$\lambda_i(A_1, \cdots, A_{i-1}, w_i, A_{i+1}, \cdots, A_m) = x/t, \quad w_j = A_j, \quad j \neq i. \tag{7.7}$$

The genuine nonlinearity of λ_i implies that the eqution (7.7) can be inverted,

$$w_i(x,t) = w_i(x/t) = \lambda_i^{-1}(x/t; A_1, \cdots, A_{i-1}, A_{i+1}, \cdots, A_m). \tag{7.8}$$

All other eigenvalues λ_j can be found as explicit functions of x/t,

$$\lambda_j = \lambda_j(A_1, \cdots, A_{i-1}, w_i(x/t), A_{i+1}, \cdots, A_m), \quad j = 1, \cdots, m, \quad j \neq i. \tag{7.9}$$

We see that these properties are exactly the same as those for the two-equation systems in Section 4. Hence we are able to treat the resolution of centered rarefaction waves in the same way, thus providing a full solution $R_i^A(x/t; U_L, U_R)$.

Next we turn to the solution of the rarefaction wave R_i in the generalized Riemann problem for the nonhomogeneous system (1.1). With the Riemann invariants as the state vector, the system (1.1) can be transformed as

$$\frac{\partial w_i}{\partial t} + \lambda_i(W)\frac{\partial w_i}{\partial x} = H_i(x, W), \quad i = 1, \cdots, m, \tag{7.10}$$

where $H_i(x, W) = Dw_i(U) \cdot S(x, U)$ and U is expressed in terms of W. In order to resolve the general rarefaction wave associated with λ_i, we fix the w_i-equation and combine a w_j-equation to form a two-equation system,

$$\begin{aligned} &\frac{\partial w_i}{\partial t} + \lambda_i\frac{\partial w_i}{\partial x} = H_i(x, W), \\ &\frac{\partial w_j}{\partial t} + \lambda_j\frac{\partial w_j}{\partial x} = H_j(x, W), \end{aligned} \tag{7.11}$$

for every $j \neq i$, $\lambda_j \neq \lambda_i$. This system is exactly the same as (4.2), w_i (resp. w_j) corresponds to ϕ (resp. ψ). We can therefore define two families of characteristic curves $C^i : \alpha_i = const.$

and $C^j : \alpha_j = const.$, respectively, by

$$\frac{dx}{dt} = \lambda_i, \qquad \frac{dx}{dt} = \lambda_j, \tag{7.12}$$

where α_i (resp. α_j) corresponds to β (resp. α) in Section 4, see Figure 4.1. We use the coordinate transforms $T_{ij} : (\alpha_i, \alpha_j) \to (x, t)$ to represent the centered rarefaction wave R_i and $T_{ij}^{ass} : (\alpha_i, \alpha_j) \to (x_{ass}, t_{ass})$ to represent the associated rarefaction wave R_i^A. In terms of these characteristic coordinates, we have characteristic equations for (7.11),

$$\begin{aligned} &\frac{\partial x}{\partial \alpha_j} = \lambda_i \frac{\partial t}{\partial \alpha_j}, \qquad \frac{\partial w_i}{\partial \alpha_j} = \frac{\partial t}{\partial \alpha_j} H_i(x, W), \\ &\frac{\partial x}{\partial \alpha_i} = \lambda_j \frac{\partial t}{\partial \alpha_i}, \qquad \frac{\partial w_j}{\partial \alpha_i} = \frac{\partial t}{\partial \alpha_i} H_j(x, W). \end{aligned} \tag{7.13}$$

We can then follow Theorem 4.3 and Eq. (4.18) in order to calculate $(\partial w_j/\partial \alpha_j)(\alpha_i, 0)$ and $(\partial t_{ass}/\partial \alpha_j)(\alpha_i, 0)$, as functions of α_i at the singularity. In fact, the following theorem is the key ingredient in our treatment of the GRP. As in the case of the linear "geometrical optics" (see Section 3) it determines the propagation of the transversal derivative of a Riemann invariant along the "degenerate" characteristic $\alpha_j = 0$ (at the origin).

Theorem 7.1. *Throughout the rarefaction wave R_i associated with λ_i connecting the head and tail values V_L and V_R, see Figure 7.1, we have*

$$\begin{aligned} &\frac{\partial t_{ass}}{\partial \alpha_j}(\alpha_i, 0) = \frac{1}{\alpha_i^L} \exp\left(\int_{\alpha_i^L}^{\alpha_i} \frac{1}{\lambda_j(\xi, 0) - \xi} d\xi \right), \\ &\frac{\partial w_j}{\partial \alpha_j}(\alpha_i, 0) = \frac{\partial w_j}{\partial \alpha_j}(\alpha_i^L, 0) + \int_{\alpha_i^L}^{\alpha_i} -\frac{H_j}{\lambda_i - \lambda_j}(\xi, 0) \cdot \frac{\partial t_{ass}}{\partial \alpha_j}(\xi, 0) d\xi, \qquad j \neq i, \end{aligned} \tag{7.14}$$

where $\alpha_i^L \le \alpha_i \le \alpha_i^R$, α_i^L and α_i^R are the speeds of the head and tail characteristics of R_i^A. The initial data is

$$\frac{\partial w_j}{\partial \alpha_j}(\alpha_i^L, 0) = w_j'(\alpha_i^L, 0) + \frac{1}{\alpha_i^L}(H_j(0, W(\alpha_i^L, 0)) - \lambda_j(\alpha_i^L, 0) w_j'(\alpha_i^L, 0)), \tag{7.15}$$

where $w_j' = \partial w_j / \partial x$.

Remark 7.2. Note that in (7.15) we have already made a choice for the characteristic coordinate α_j, the value α_j is the $x-$coordinate of the intersection point of the characteristic curve with the head characteristic of R_i. Of course, other convenient choices are also possible.

Following Theorem 7.1, we express

$$\begin{aligned} \frac{\partial w_j}{\partial \alpha_j}(\alpha_i^R, 0) &= \left(\frac{\partial w_j}{\partial t}(\alpha_i^R, 0) + \lambda_i^R \frac{\partial w_j}{\partial x}(\alpha_i^R, 0) \right) \cdot \frac{\partial t_{ass}}{\partial \alpha_j}(\alpha_i^R, 0) \\ &= \left(\frac{\lambda_j^R - \lambda_i^R}{\lambda_j^R} \cdot \frac{\partial w_j}{\partial t}(\alpha_i^R, 0) + \frac{\lambda_i^R}{\lambda_j^R} \cdot H_j(0, W(\alpha_i^R, 0)) \right) \cdot \frac{\partial t_{ass}}{\partial \alpha_j}(\alpha_i^R, 0), \end{aligned} \tag{7.16}$$

where we have used (7.11) and the smoothness of w_j. Translating the result of Theorem 7.1 to the (x,t)-coordinate at the tail characteristic $\alpha_i = \alpha_i^R$, we obtain the following theorem.

Theorem 7.3. *Assume that the rarefaction wave R_i associated with λ_i connects the states V_L and V_R. Let α_i^L and α_i^R be the corresponding characteristic speeds at the head and tail of R_i^A, respectively. Let Dw_j be as in (7.3) and denote by $(\partial U/\partial t)_R$ the value evaluated at the tail characteristic $\alpha_i = \alpha_i^R$ from the smooth region behind R_i. Then one obtains,*

$$(Dw_j)_R \left(\frac{\partial U}{\partial t}\right)_R = d_{LR}^j, \qquad j \neq i, \tag{7.17}$$

where the constant term d_{LR}^j is expressed as

$$d_{LR}^j = \frac{\lambda_j^R}{\lambda_j^R - \lambda_i^R}\left(\frac{\partial w_j}{\partial \alpha_j}(\alpha_i^R, 0)\left(\frac{\partial t_{ass}}{\partial \alpha_j}\right)^{-1}(\alpha_i^R, 0) - \frac{\lambda_i^R}{\lambda_j^R} H_j(0, W(\alpha_i^R, 0))\right), \tag{7.18}$$

and $\lambda_j^R = \lambda_j(\alpha_i^R, 0)$ and $\lambda_i^R = \alpha_i^R$.

Proof. Note that the limiting value of $\partial w_j/\partial t$ is obtained by Eq. (7.16). Now we use the chain rule for the values in the smooth region behind R_i to obtain (7.17). □

Remark 7.4. (Degenerate rarefaction wave or acoustic wave). Note that in the resolution of GRP, all waves must be accounted for. In particular, the $i-$th wave can just be a characteristic curve, which we regard as a degenerate rarefaction wave or an acoustic wave $\alpha_i^R = \alpha_i^L$. All variables w_j, $j = 1, \cdots, m$, are continuous, but in this case $\partial w_i/\partial t$, $\partial w_i/\partial x$ may experience a jump.

We now proceed to the general derivation of the limiting values (1.6) for the generalized Riemann problem (1.1) and (2.1). We first illustrate this by considering a special case. Assume that the associated Riemann problem (2.3) and (2.4) has a solution of m rarefaction waves which separate $m+1$ constant states, cf. Figure 7.1. Let the t-axis be located inside the intermediate region between the i-rarefaction wave and the $i+1$-rarefaction wave. Then we have the following proposition.

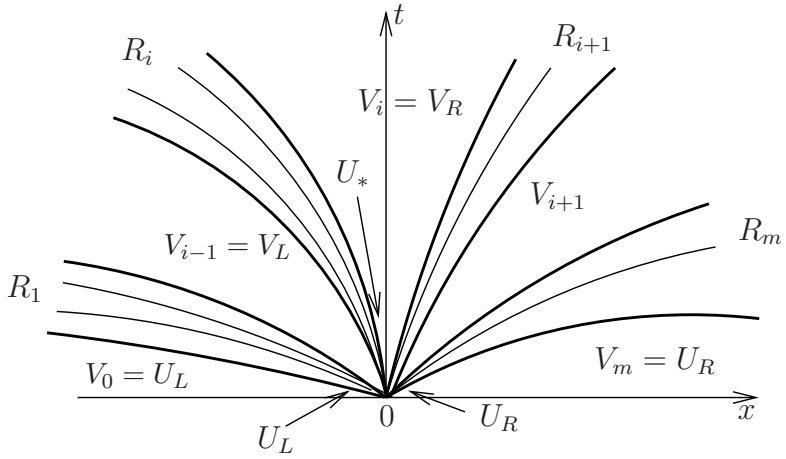

FIGURE 7.1. Wave configuration for the generalized Riemann problem

Proposition 7.5. *Assume that the Riemann solution of (1.1) and (2.1) only consists of m rarefaction waves and that the t-axis is located inside the intermediate region between the i-th rarefaction wave and the $i+1$-st rarefaction wave. Then $(\partial U/\partial t)_*$ can be obtained through the following system of linear algebraic equations,*

$$\sum_{k=1}^{m} a_{jk}\left(\frac{\partial u_k}{\partial t}\right)_* = d_j, \qquad j = 1, \cdots, m, \tag{7.19}$$

where $(a_{j1}, \cdots, a_{jm}) = (Dw_j)_*$, and d_j, $j = 1, \cdots, m$, are constants only depending on the initial data (2.1) and the Riemann solution $R^A(\cdot; U_L, U_R)$.

Proof. We label by $I_0, I_1, \cdots, I_m$ the regions corresponding to the constant state regions in the associated Riemann problem from the left to the right, as in Figure 7.1. We start from the first rarefaction wave associated with λ_1. By Theorem7.3, we can obtain the directional derivatives for w_j, $j = 2, \cdots, m$ in the region I_1 across this first rarefaction wave. Successively, we can calculate the derivatives of w_j, $j = k+1, \cdots, m$ across the λ_k-rarefaction wave, $k \le i$, up to the λ_i-rarefaction wave. Consequently we obtain in the region I_i,

$$\sum_{k=1}^{m} a_{jk}\left(\frac{\partial u_k}{\partial t}\right)_* = d_j, \quad j = i+1, \cdots, m, \tag{7.20}$$

from the left-hand side.

Similarly, we start from the region I_m for the λ_m-th rarefaction wave in the right hand side to get the solution w_j, $j = 1, \cdots, m-1$, in the region I_{m-1}. Successively, we obtain in the region I_i,

$$\sum_{k=1}^{m} a_{jk}\left(\frac{\partial u_k}{\partial t}\right)_* = d_j, \quad j = 1, \cdots, i. \tag{7.21}$$

We combine (7.20) and (7.21) to obtain (7.19). Note that $(a_{j1}, \cdots, a_{jm}) = (Dw_j)_*$. The system (7.19) is uniquely solvable. □

Remark 7.6. The process of proof actually yields a constructive approach to the calculation of the instantaneous values of time-derivatives along the t-axis.

As pointed out at the beginning of this section, the system (1.1) is in general not endowed with a coordinate system of Riemann invariants. However, we can still use the concept of the Riemann invariants, as a main ingredient, in the treatment of rarefaction waves for a *weakly coupled system*, which we define next.

We denote by $L_i(U)$ the left eigenvector associated with λ_i and by $L(U)$ the left eigenmatrix whose i-th row vector is $L_i(U)$. Then we multiply (1.1) from the left by $L(U)$ to get

$$L(U)\frac{\partial U}{\partial t} + \Lambda(U)L(U)\cdot\frac{\partial U}{\partial x} = L(U)S(x,U), \tag{7.22}$$

where $\Lambda(U)$ is a diagonal matrix with diagonal entries λ_i. Set

$$W = L(U)U. \tag{7.23}$$

Then (7.22) can be written as

$$\frac{\partial W}{\partial t}+\Lambda(U)\frac{\partial W}{\partial x}=\Pi\left(\frac{\partial U}{\partial t},\frac{\partial U}{\partial x}\right)+\overline{S}(x,U), \tag{7.24}$$

where

$$\Pi\left(\frac{\partial U}{\partial t},\frac{\partial U}{\partial x}\right)=\left[\frac{\partial L(U)}{\partial t}+\Lambda(U)\frac{\partial L(U)}{\partial x}\right]U,\quad \overline{S}(U)=L(U)\cdot S(x,U). \tag{7.25}$$

In general, Π does not vanish. However, suppose that we can split the vector of unknowns W into two parts, $W=(W^a,W^b)^\top$, so that the system (7.24) can be decoupled into two subsystems

$$\begin{aligned}(S_a):&\quad \frac{\partial W^a}{\partial t}+\Lambda^a(U)\frac{\partial W^a}{\partial x}=\Pi^a\left(\frac{\partial U}{\partial t},\frac{\partial U}{\partial x}\right)+\overline{S}^a(x,U),\\ (S_b):&\quad \frac{\partial W^b}{\partial t}+\Lambda^b(U)\frac{\partial W^b}{\partial x}=\Pi^b\left(\frac{\partial U}{\partial t},\frac{\partial U}{\partial x}\right)+\overline{S}^b(x,U),\end{aligned} \tag{7.26}$$

which satisfy

(i) $\Pi^b=0$.
(ii) Π^a does not depend on the derivatives of W^a.
(iii) $\Lambda^a(U)$ and $\Lambda^b(U)$ are diagonal matrices, and

$$\Lambda(U)=\begin{pmatrix}\Lambda^a(U) & 0\\ 0 & \Lambda^b(U)\end{pmatrix}. \tag{7.27}$$

Thus we can first resolve the rarefaction waves corresponding to the subsystem (S_b) for W^b and then resolve the system (S_a) for W^a, using the same methodology as in the last subsection. This is the family of *weakly coupled* systems we define below.

Definition 7.7. We say that the system (1.1) is *weakly coupled* if there is a coordinate system of *quasi-Riemann invariants* $W(U)=(W^a(U),W^b(U))^\top$ such that (1.1) can be reduced to the *quasi-diagonal* form,

$$\begin{cases}\dfrac{\partial W^a}{\partial t}+\Lambda^a(W)\dfrac{\partial W^a}{\partial x}=\Pi^a\left(W,\dfrac{\partial W^b}{\partial x}\right)+K^a(x,W),\\[2ex] \dfrac{\partial W^b}{\partial t}+\Lambda^b(W)\dfrac{\partial W^b}{\partial x}=K^b(x,W),\end{cases} \tag{7.28}$$

where Λ^a and Λ^b are diagonal matrices and their entries are the eigenvalues of DF.

For convenience, we denote

$$\Lambda(W)=\begin{pmatrix}\Lambda^a(W) & 0\\ 0 & \Lambda^b(W)\end{pmatrix},\quad \Pi=\begin{pmatrix}\Pi^a\\ 0\end{pmatrix},\quad K=\begin{pmatrix}K^a\\ K^b\end{pmatrix}, \tag{7.29}$$

and (7.28) is written as

$$\frac{\partial W}{\partial t}+\Lambda(W)\frac{\partial W}{\partial x}=\Pi\left(W,\frac{\partial W^b}{\partial x}\right)+K(x,W). \tag{7.30}$$

As we shall show later the system of compressible fluid flow is an important example of a weakly coupled system. Also, all systems that can be transformed into a form involving upper triangular coefficient matrix are weakly coupled. Indeed, in this case the above splitting is into m scalar equations, where the solution procedure resembles the Gaussian elimination. As a result, our problem boils down to solving the diagonal system (7.10).

7.2. **Remarks on the sonic case.** As in Subsection 6.1, we need to deal with the sonic case that the t-axis is tangential to the i-characteristic at the origin $(x,t)=(0,0^+)$ for some i. It is clear that Theorem 7.3 still holds, where α_i^R is replaced by $\alpha_i=0$. In addition, we use the w_i-equation in (7.10), by noting the fact that $\lambda_i(W^0)=0$, $W^0=W(\alpha_i=0,\alpha_j=0)$, to get

$$\left(\frac{\partial w_i}{\partial t}\right)\Big|_{(\alpha_i,\alpha_j)=(0,0)}=H_i(0,W^0). \tag{7.31}$$

It follows that

$$(Dw_i)_0\left(\frac{\partial U}{\partial t}\right)_*=H_i(0,W^0). \tag{7.32}$$

We summarize these facts in the following theorem (cf. Theorem 6.2).

Theorem 7.8. *Assume that the t-axis is located in the rarefaction wave associated with the eigenvalue λ_i. Then $(\partial U/\partial t)_*$ is determined by a system of m linear equations; the $m-1$ equations are given in (7.17) with $\alpha_i^R=0$, and the other one is given by (7.32).*

7.3. **The resolution of jump discontinuities.** We use the same approach as in Section 5 in order to resolve the jump discontinuity (shock or contact discontinuity) for general systems. Let the jump location be given by $x=x(t)$ with speed $\sigma(t)=x'(t)$. This jump discontinuity is described by the Rankine-Hugoniot jump condition,

$$F(U)-F(\overline{U})=\sigma(U-\overline{U}), \tag{7.33}$$

where U and $\overline{U}$ are the limiting states on two sides, respectively. Let us fix the state $\overline{U}$. Then (7.33) is the system of the size m but with $m+1$ unknowns U and σ. As a standard approach [8], we write (7.33) as

$$\left[A(U,\overline{U})-\sigma I\right](U-\overline{U})=0, \tag{7.34}$$

where we are using the Roe matrix

$$A(U,\overline{U})=\int_0^1 DF(\tau U+(1-\tau)\overline{U})d\tau. \tag{7.35}$$

Solving (7.34) yields,

$$\begin{cases}\sigma=\sigma_i(U,\overline{U}),\\ U=\overline{U}+\eta\Gamma_i(U,\overline{U}),\end{cases} \tag{7.36}$$

for a parameter $\eta \in \mathbb{R}$, where the i-th jump discontinuity speed σ_i is the eigenvalue of $A(U, \overline{U})$, and Γ_i is the associated eigenvector, $i = 1, \cdots, m$.

For a fixed i-jump discontinuity, we eliminate η in (7.36) to get $m-1$ equations,

$$\Psi_i^j(U, \overline{U}) = 0, \qquad j = 1, \cdots, m-1. \tag{7.37}$$

Indeed, this is the system determining the i-th Hugoniot locus in the U space. We differentiate these equations in the direction of the jump discontinuity $x = x(t)$, $x'(t) = \sigma_i(U, \overline{U})$, to get

$$\nabla_U \Psi_i^j(U, \overline{U}) \cdot \left(\frac{\partial U}{\partial t} + \sigma_i \frac{\partial U}{\partial x} \right) = -\nabla_{\overline{U}} \Psi_i^j(U, \overline{U}) \cdot \left(\frac{\partial \overline{U}}{\partial t} + \sigma_i \frac{\partial \overline{U}}{\partial x} \right). \tag{7.38}$$

Denote the limiting values of σ_i, U, $\overline{U}$, $\partial U/\partial t$ and $\partial \overline{U}/\partial x$ as t tends to zero by

$$\lim_{t \to 0^+} \sigma_i = \sigma_i^0, \quad \lim_{t \to 0^+} U = U_l, \quad \lim_{t \to 0^+} \overline{U} = U_r, \quad \lim_{t \to 0^+} \frac{\partial U}{\partial t} = \left(\frac{\partial U}{\partial t} \right)_l, \quad \lim_{t \to 0^+} \frac{\partial \overline{U}}{\partial x} = U_r'. \tag{7.39}$$

We suppose that the jump discontinuity moves to the right so that $\sigma_i(U_l, U_r) > 0$. Our goal is to seek $(\partial U/\partial t)_l$. Using (1.1) for smooth solutions, we replace the time derivative $\partial \overline{U}/\partial t$ by the spatial derivative $\partial \overline{U}/\partial x$ and replace the spatial derivative $\partial U/\partial x$ by the time derivative $\partial U/\partial t$,

$$\begin{aligned} \frac{\partial \overline{U}}{\partial t} &= -DF(\overline{U}) \frac{\partial \overline{U}}{\partial x} + S(x, \overline{U}), \\ \frac{\partial U}{\partial x} &= DF(U)^{-1} \left[-\frac{\partial U}{\partial t} + S(x, U) \right], \end{aligned} \tag{7.40}$$

where we assume that $DF(U_l)$ is invertible. The case that $DF(U_l)$ is singular is discussed below in the context of quasi-Riemann invariants. Inserting these relations in (7.38) and taking the time limit we get, for $j = 1, ..., m-1$,

(7.41)

$$\begin{aligned} &\nabla_U \Psi_i^j(U_l, U_r)[I - \sigma_i^0 DF(U_l)^{-1}] \left(\frac{\partial U}{\partial t} \right)_l \\ = \; & -\sigma_i^0 \nabla_U \Psi_i^j(U_l, U_r) DF(U_l)^{-1} S(0, U_l) - \nabla_{\overline{U}} \Psi_i^j(U_l, U_r) \left[(\sigma_i^0 I - DF(U_r)) U_r' + S(0, U_r) \right]. \end{aligned}$$

Note that this is a system of $m-1$ linearly independent algebraic equations with m unknowns $(\partial U/\partial t)_l$. This leads to the following theorem for the resolution of the i-shock.

Theorem 7.9. *Let the jump discontinuity $x = x(t)$ be associated with the eigenvalue λ_i, the related limiting states are denoted in (7.39). Then at the singularity point $(x, t) = (0, 0)$ we have*

$$\sum_{q=1}^{m} a_{iq}^j \left(\frac{\partial u_q}{\partial t} \right)_l = d_i^j, \qquad j = 1, \cdots, m-1, \tag{7.42}$$

where all coefficients a^j_{iq} and d^j_i are given explicitly by,

(7.43)
$$(a^j_{i1}, \cdots, a^j_{im}) = \nabla_U \Psi^j_i(U_l, U_r)[I - \sigma^0_i DF(U_l)^{-1}]$$

$$d^j_i = -\sigma^0_i \nabla_U \Psi^j_i(U_l, U_r) DF^{-1}(U_l) S(0, U_l) - \nabla_{\overline{U}} \Psi^j_i(U_l, U_r) \left[(\sigma^0_i I - DF(U_r))U'_r + S(0, U_r)\right].$$

Now we turn to the case of a weakly coupled system (7.30), as in Definition 7.7, and work with the quasi-Riemann invariants $W = (w_1, \cdots, w_m)$. Then (7.37) can be written as

$$\Phi^j_i(W; \overline{W}) = 0, \quad j = 1, \cdots, m-1. \tag{7.44}$$

We use the same approach as above to differentiate (7.44) in the direction of the jump discontinuity $x = x(t)$, express $\partial W/\partial x$ by $\partial W/\partial t$ and $\partial \overline{W}/\partial t$ by $\partial \overline{W}/\partial x$ using (7.30),

$$\nabla_W \Phi^j_i \cdot \left(\frac{\partial W}{\partial t} + \sigma_i \frac{\partial W}{\partial x}\right) = -\nabla_{\overline{W}} \Phi^j_i \cdot \left(\frac{\partial \overline{W}}{\partial t} + \sigma_i \frac{\partial \overline{W}}{\partial x}\right),$$

$$\frac{\partial W}{\partial x} = \Lambda(W)^{-1} \cdot \left[-\frac{\partial W}{\partial t} + \overline{\Pi}(W, \frac{\partial W^b}{\partial t}) + K(x, W)\right], \tag{7.45}$$

$$\frac{\partial \overline{W}}{\partial t} = -\Lambda(\overline{W}) \cdot \frac{\partial \overline{W}}{\partial x} + \Pi(\overline{W}, \frac{\partial \overline{W}^b}{\partial x}) + K(x, \overline{W}),$$

where $\overline{\Pi}(W, \partial W^b/\partial t) = \Pi(W, \Lambda^b(W)^{-1} \cdot (-\frac{\partial W^b}{\partial t} + K^b(x, W)))$, and non-zero eigenvalues are assumed. Indeed, once some eigenvalue λ_k ($k \neq i$) is zero in the limit $t \to 0^+$, we have from (7.30),

$$\frac{\partial w_k}{\partial t} = \Pi_k \left(W, \frac{\partial W^b}{\partial x}\right) + K_k(x, W), \quad k \neq i. \tag{7.46}$$

Then the limiting value of $\partial w_k/\partial t$ is known, and we just need to consider the reduced (7.45) in terms of the other variables w_j, $j \neq k$. For the simplicity in presentation, we therefore assume that all eigenvalues are not zero. Incorporating the last two identities of (7.45) into the first one, we have,

$$\begin{aligned} & \nabla_W \Phi^j_i \left[(I - \sigma_i \Lambda(W)^{-1}) \frac{\partial W}{\partial t} + \sigma_i \Lambda(W)^{-1} \cdot \overline{\Pi}(W, \frac{\partial W^b}{\partial t})\right] \\ = \; & -\nabla_W \Phi^j_i \cdot \sigma_i \cdot \Lambda(W)^{-1} \cdot K(x, W) \\ & -\nabla_{\overline{W}} \Phi^j_i \left[(\sigma_i I - \Lambda(\overline{W})) \frac{\partial \overline{W}}{\partial x} + K(x, \overline{W}) + \Pi(W, \partial W^b/\partial x)\right]. \end{aligned} \tag{7.47}$$

By taking the limit $t \to 0^+$, we obtain (in analogy to (7.41)),

$$\begin{aligned}
&\nabla_W \Phi_i^j(W_l, W_r) \left[(I - \sigma_i^0 \Lambda(W_l)^{-1}) \left(\frac{\partial W}{\partial t} \right)_l + \sigma_i^0 \Lambda(W_l)^{-1} \cdot \overline{\Pi} \left(W_l, \left(\frac{\partial W^b}{\partial t} \right)_l \right) \right] \\
&= -\nabla_W \Phi_i^j(W_l, W_r) \cdot \sigma_i^0 \cdot \Lambda(W_l)^{-1} \cdot K(0, W_l) \qquad (7.48) \\
&\quad -\nabla_{\overline{W}} \Phi_i^j(W_l, W_r) \left[(\sigma_i^0 I - \Lambda(W_r)) W_r' + K(0, W_r) + \Pi(W_r, (W_r^b)') \right].
\end{aligned}$$

This is a system of $m-1$ algebraic equations with m unknowns $(\partial w_k/\partial t)_l$, $k = 1, \cdots, m$. Note that the i-th term of the matrix $I - \sigma_i^0 \Lambda(W_l)^{-1}$ may be zero. Therefore we let $(\partial w_i/\partial t)_l$ be a free undetermined parameter, and we obtain a system of $m-1$ equations for the limiting values $(\partial w_k/\partial t)_l$, $k \neq i$, which is given by the following theorem.

Theorem 7.10. *Consider the weakly coupled system (7.30). Let the jump discontinuity $x = x(t)$ be associated with λ_i, $\sigma_i^0 = x'(0) > 0$. Then at the singularity point $(x, t) = (0, 0)$, we have the following connections between the vector $(\partial W/\partial t)_l$ of time derivatives on the left hand side of the jump discontinuity and the spatial derivatives $W_r' := (\partial W/\partial x)_r$ on the right hand side,*

$$\sum_{q=1}^{m} \frac{\partial \Phi_i^j}{\partial w_q} \cdot \frac{\lambda_q(W_l) - \sigma_i^0}{\lambda_q(W_l)} \cdot \left(\frac{\partial w_q}{\partial t} \right)_l + \sum_{q=1}^{m} \frac{\partial \Phi_i^j(W_l, W_r)}{\partial w_q} \cdot \frac{1}{\lambda_q(W_l)} \cdot \overline{\Pi}_q(W_l, \left(\frac{\partial W^b}{\partial t} \right)_l) = d_i^j, \qquad (7.49)$$

where $j = 1, \cdots, m-1$, and d_i^j are given explicitly by,

$$\begin{aligned}
d_i^j = \; & -\textstyle\sum_{q=1}^{m} \dfrac{\partial \Phi_i^j(W_l, W_r)}{\partial w_q} \cdot \dfrac{\sigma_i^0}{\lambda_q(W_l)} \cdot K_q(0, W_l) \\
& -\textstyle\sum_{q=1}^{m} \dfrac{\partial \Phi_i^j(W_l, W_r)}{\partial \overline{w}_q} \cdot \left[(\sigma_i^0 - \lambda_q(W_r)) W_r' + K_q(0, W_r) + \Pi_q(W_r, (W_r^b)') \right].
\end{aligned} \qquad (7.50)$$

The system (7.49) is an algebraic system for $(\partial w_k/\partial t)_l$, $k \neq i$, with the value $(\partial w_i/\partial t)_l$ being an independent parameter.

Remark 7.11. Theorems 7.9 and 7.10 show that we can either use the primitive variables U or the quasi-Riemann invariants W for weakly coupled systems in resolving jump discontinuities. The choice of either approach depends on the practical convenience.

Remark 7.12. (Weak jump). As in Remark 7.4, in the limit that the strength of the $i-$th shock becomes zero ($W_l = W_r$), the shock trajectory $x = x(t)$ degenerates to a characteristic curve and $\lambda_i(W_l) = \sigma_i^0 = \lambda_i(W_r)$. The term containing $(\partial w_i/\partial t)_l$ is kicked out in (7.49). Finally we get $(\partial w_j/\partial t)_l = (\partial w_j/\partial t)_r$ and $(\partial w_j/\partial x)_l = (\partial w_j/\partial x)_r$, $j \neq i$. However, $(\partial w_i/\partial t)_l \neq (\partial w_i/\partial t)_r$.

7.4. **Remarks on the resolution of contact discontinuities.** In the last subsection we have resolved the jump discontinuities, including contact discontinuities associated with linearly degenerate eigenvalues. However, when the system (1.1) is endowed with a coordinate system of Riemann invariants, as written in (7.10), the situation becomes much simpler for contact discontinuities.

Assume that the eigenvalue λ_i is linearly degenerate and the corresponding contact discontinuity is $x = x(t)$. By the definition of Riemann invariants, see (7.3), we see that the Riemann invariant w_j, associated with λ_i, is continuous across the contact discontinuity $x = x(t)$, $x'(t) = \sigma_i(U, \overline{U}) = \lambda_i(U) = \lambda_i(\overline{U})$,

$$w_j(U) = w_j(\overline{U}), \quad j \neq i. \tag{7.51}$$

Using the same approach as in the last subsection, we differentiate w_j in the direction of $x = x(t)$ to yield

$$\frac{\partial w_j(U)}{\partial t} + \lambda_i(U)\frac{\partial w_j(U)}{\partial x} = \frac{\partial w_j(\overline{U})}{\partial t} + \lambda_i(\overline{U})\frac{\partial w_j(\overline{U})}{\partial x}. \tag{7.52}$$

Using (7.10), we have

$$\begin{aligned} \frac{\partial w_j(U)}{\partial x} &= \frac{1}{\lambda_j(U)}\left[-\frac{\partial w_j(U)}{\partial t} + H_j(x, W(U))\right], \\ \frac{\partial w_j(\overline{U})}{\partial t} &= -\lambda_j(\overline{U})\frac{\partial w_j(\overline{U})}{\partial x} + H_j(x, W(\overline{U})). \end{aligned} \tag{7.53}$$

Note that if $\lambda_j(U) = 0$, $(\partial w_j/\partial t)_l = H(0, W_l)$, and we do not need the above manipulation. Thus we assume that $\lambda_j(U_l) \neq 0$ so that we use (7.53) in (7.52) and take the time limit to obtain (see (7.39) for notations),

$$\left(\frac{\partial w_j}{\partial t}\right)_l := \frac{\lambda_j^l}{\lambda_j^l - \lambda_i^l}\left[(\lambda_i^r - \lambda_j^r)(w_j)_r' + H_j(0, W_r) - \frac{\lambda_i^l}{\lambda_j^l}H_j(0, W_l))\right], \tag{7.54}$$

where $\lambda_j^l = \lambda_j(U_l)$, $(w_j)_r' = (\partial w_j/\partial x)_r$ etc. Thus we obtain the time derivative $(\partial w_j/\partial t)_l$ provided that $(w_j)_r'$ and the associated Riemann solution are known. Then the time derivative $(\partial U/\partial t)_l$ follows. We summarize the above to give the following theorem.

Theorem 7.13. *Let the contact discontinuity $x = x(t)$ be associated with λ_i and separate two limiting states W_l and W_r. Then we have*

$$Dw_j(U_l) \cdot \left(\frac{\partial U}{\partial t}\right)_l = d_j^{rl}, \quad j \neq i, \tag{7.55}$$

where the quantity d_j^{rl} is expressed explicitly as

$$d_j^{rl} = \frac{\lambda_j^l}{\lambda_j^l - \lambda_i^l}\left[(\lambda_i^r - \lambda_j^r)(w_j)_r' + H_j(0, W_r) - \frac{\lambda_i^l}{\lambda_j^l}H_j(0, W_l)\right]. \tag{7.56}$$

7.5. **The time derivative of solutions at the singularity.** In this final subsection we wrap up the calculation of the GRP solution $(\partial U/\partial t)_*$, see (2.2). We assume that the rarefaction waves, shocks and contact discontinuities can be resolved with the approach in Subsections 7.1–7.4, and that the local wave pattern at the origin, determined by the associated Riemann solution of (2.3) and (2.4), consists of m waves. If the t-axis is located on one side of all waves, the value of $(\partial U/\partial t)_*$ can be obtained upwind. Therefore, we assume that the t-axis is located inside the intermediate region between the i-th wave and $(i+1)$-st wave. The strategy of the computation of $(\partial U/\partial t)_*$ is analogous to Proposition 7.5, but at

present, the treatment depends on the type of the j-th wave ($j = 1, \cdots, m$); a rarefaction wave, a shock or a contact discontinuity. As has been pointed out, the local wave pattern is determined by the associated Riemann solution $R^A(x/t; U_L, U_R)$, see Proposition 2.1.

Theorem 7.14. *The limiting value $(\partial U/\partial t)_*$ can be obtained by solving the following system of linear algebraic equations*

$$\sum_{k=1}^{m} a_{jk} \left(\frac{\partial u_k}{\partial t} \right)_* = d_j, \quad j = 1, \cdots m, \tag{7.57}$$

where the coefficients a_{jk} and d_j are explicitly determined by the initial data (2.1) and the associated Riemann solution $R^A(0; U_L, U_R)$.

Proof. The basic idea of the proof, and, indeed, the cornerstone of the GRP methodology, is identical to that of Proposition 7.5, where all m waves were assumed to be rarefaction wave. In fact, the initial slopes (2.1) are "rotated" through the various waves emanating from the origin so as to yield the desired $(\frac{\partial U}{\partial t})_*$. We first observe that the results of Subsection 7.1 (rarefaction waves) and Subsections 7.3-7.4 (jump discontinuities) can be summarized as follows. Given the limiting values (at $(x,t) = (0,0)$) of the temporal and spatial derivatives of the unknowns (expressed either by U or the quasi-Riemann invariants W) on one side of the discontinuity, we find $(m-1)$ equations for the (limiting values of the) temporal derivatives on the other side (the spatial derivatives are then obtained from the system (1.1)). In other words,"crossing" a single wave we are left with one free parameter in a system of m equations for the derivatives (on the side labelled as "unknown"). Suppose now that the $t-$axis is located between the i-th and $(i+1)$-st waves. Counting from the left ($x < 0$) we get for $(\frac{\partial U}{\partial t})_*$ a system of m equations, with i free parameters. Similarly, approaching from the right ($x > 0$) we cross $(m-i)$ waves, and thus get another system of m equations, containing $(m-i)$ free parameters. Eliminating the total of m free parameters from the two systems of m equations we obtain precisely the system claimed in the theorem.

Note that in the sonic case, where the t-axis is "imbedded" in a rarefaction wave, the proof is simpler and the full system is determined by the data on one side.

To illustrate our procedure, we examine a few examples in the case of a system of four equations ($m = 4$). The use of quasi-Riemann invariants enables us to simplify the general procedure above (with free parameters) as follows. First we consider a degenerate example of two waves, as in Figure 7.2: A shock associated with λ_1 moves to the left and a rarefaction wave associated with λ_4 moves to the right, the dashed curves represent the acoustic waves associated with λ_3 and λ_4, respectively. Applying Theorem 7.3, we get the limiting values of the derivatives for w_1, w_2 and w_3 in the region I_4 by resolving the 4-rarefaction wave. Note (Remarks 7.4 and 7.12) that out of these derivatives only the derivatives of w_1 and w_2 are continuous across the 3-acoustic wave. Hence we get the limiting values $(\partial w_1/\partial t)_*$ and $(\partial w_2/\partial t)_*$ in the region I_3. On the other hand, across the $1-$shock we have three equations for the limiting values of four unknowns $\partial w_i/\partial t$, $i = 1, 2, 3, 4$, in the region I_2, see Theorem 7.10. Since the derivatives of w_1, w_3 and w_4 are continuous across the 2-acoustic wave and $(\partial w_1/\partial t)_*$ is already known, we can solve the three equations for the limiting values of the unknowns $\partial w_i/\partial t$, $i = 2, 3, 4$, in the region I_2. Then these limiting values for $i = 3, 4$ are equal to $(\partial w_3/\partial t)_*$ and $(\partial w_4/\partial t)_*$ in the region I_3, respectively.

The second example consists of two shocks, as in Figure 7.3. In this case the 4-rarefaction wave of the previous example is replaced by a 4-shock. We use Theorem 7.10 (see (7.49))

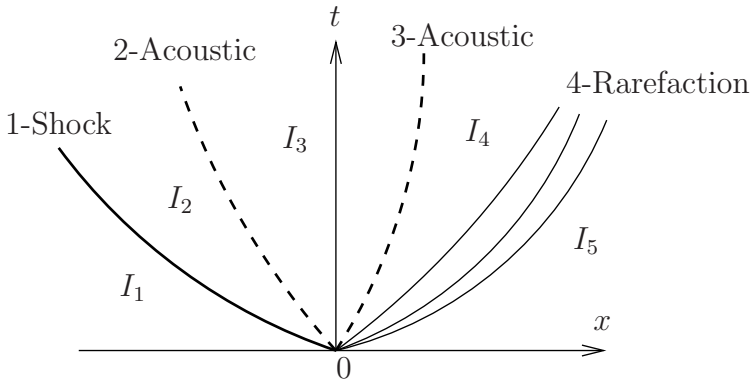

FIGURE 7.2. An example for a two–wave degenerate pattern for four-equation system: A shock of first family wave moves to the left and a rarefaction wave of fourth family moves to the right.

to obtain three equations for the limiting values of the four unknowns $\partial w_i/\partial t$ in the region I_2 by resolving the 1−shock, and another set of three equations for the limiting values of the four unknowns $\partial w_i/\partial t$ in the region I_4 by resolving the 4−shock, $i = 1, 2, 3, 4$. Since $\partial w_i/\partial t$, $i = 1, 3, 4$, are continuous across the 2−acoustic wave and $\partial w_i/\partial t$, $i = 1, 2, 4$, are continuous across the 3−acoustic wave, we finally obtain six equations with the four unknowns $(\partial w_i/\partial t)_*$, $i = 1, 2, 3, 4$, in the region I_3 and the other two unknown limiting values $\partial w_2/\partial t$ in the region I_2 and $\partial w_3/\partial t$ in the region I_4.

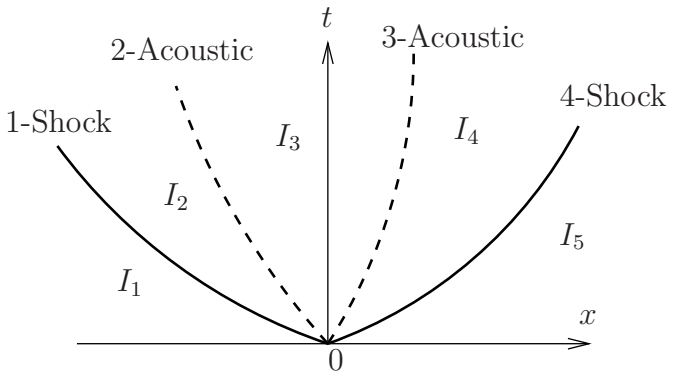

FIGURE 7.3. An example for a two-wave degenerate pattern for four-equation system: Two shocks of first and fourth families move to the left and right, respectively.

We assume for the third example, as in Figure 7.4, that the local wave configuration consists of four waves: Two rarefaction waves propagate to the right, a rarefaction wave and a shock move to the left, the t-axis is located in the intermediate region I_3. With the results in Subsection 7.1, we can get the limiting values of $\partial w_1/\partial t$, $\partial w_2/\partial t$ and $\partial w_3/\partial t$ in the region I_4 by resolving the 4-rarefaction wave. Then the limiting values of $\partial w_1/\partial x$, $\partial w_2/\partial x$ and $\partial w_3/\partial x$ are obtained by using (7.10). We continue to resolve the 3-rarefaction wave to get the limiting value $(\partial w_1/\partial t)_*$ and $(\partial w_2/\partial t)_*$ in the intermediate region I_3. Analogously, we can resolve the 1-rarefaction wave from the left-hand side to get the limiting values of $\partial w_2/\partial t$, $\partial w_3/\partial t$ and $\partial w_4/\partial t$ (resp. the limiting values of $\partial w_2/\partial x$, $\partial w_3/\partial x$ and $\partial w_4/\partial x$

again by using (7.10)) in the region I_2. Then we proceed to resolve the 2-shock to obtain $(\partial w_3/\partial t)_*$ and $(\partial w_4/\partial t)_*$ in the intermediate region I_3. Recall (Theorem 7.10) that there are three equations connecting the limiting values of derivatives of w_i, $i = 1, 2, 3, 4$. Note that the limiting values of the derivatives for w_2, w_3 and w_4 in the region I_2 are determined by the treatment of the 1-rarefaction wave, leaving there the limiting value of $\partial w_1/\partial t$ as a free parameter. Using the (already known) limiting values $(\partial w_1/\partial t)_*$ and $(\partial w_2/\partial t)_*$ in the region I_3, we have three equations for three unknowns; the limiting value of $\partial w_1/\partial t$ in the region I_2 as well as $(\partial w_3/\partial t)_*$ and $(\partial w_4/\partial t)_*$ in the region I_3. Solving these we get $(\partial w_3/\partial t)_*$ and $(\partial w_4/\partial t)_*$ in I_3.

Once we solve the resulting system of linear equations to get $(\partial w_i/\partial t)_*$, $i = 1, 2, 3, 4$, we immediately obtain $(\partial U/\partial t)_*$ in the intermediate region I_3.

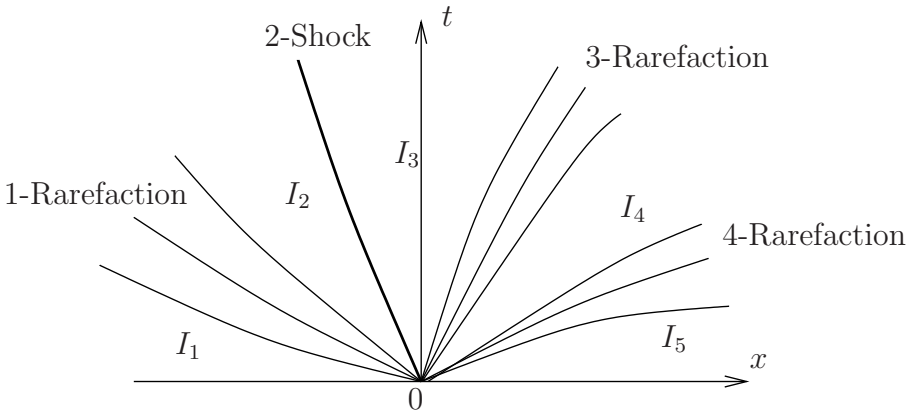

FIGURE 7.4. An example for a full four-wave pattern for four-equation system: Two rarefaction waves move to the right, and a rarefaction wave and a shock move to the left.

□

8. The acoustic approximation and the G_1-scheme

The acoustic approximation makes sense if the jump at the singularity point $(x, t) = (0, 0)$ is sufficiently small. Assume that the initial variables $U(x, 0)$ in (2.1) are continuous at $x = 0$ while their slopes are not; $U_L = U_R$ and $U'_L \neq U'_R$. Then the Riemann solution to the associated Riemann problem is constant $R^A(x/t; U_L, U_R) \equiv U_L = U_R$. Therefore the initial wave pattern does not contain a jump discontinuity (shock) or a centered rarefaction wave. The "waves" emanating from the origin $(x, t) = (0, 0)$ are acoustic, and therefore their speeds are $\lambda_i(U_L) = \lambda_i(U_R)$, $i = 1, \cdots, m$.

Denote $U_* = U_L = U_R$. Then we can linearize (1.1) around $U = U_*$ to get

$$\frac{\partial U}{\partial t} + DF(U_*)\frac{\partial U}{\partial x} = S(x, U_*). \tag{8.1}$$

With this linear system of equations, we can use the customary methods, as in Section 3, to get the derivative $(\partial U/\partial t)_*$: Diagonalize the system (8.1), calculate the derivatives upwind and return to the primitive variables $(\partial U/\partial t)_*$.

In our GRP scheme, the initial data (2.1) has a jump discontinuity, and we can solve the generalized Riemann problem (1.1) and (2.1) analytically to calculate the time derivative of

solution, as has been summarized in Subsection 7.5. This leads to the scheme which we label as the G_∞ *scheme.*

In practice, when $U_L - U_R$ is sufficiently small, we can simplify this process by resorting to the acoustic case. Setting the Riemann solution $U_* = R^A(0; U_L, U_R)$ as the background solution, we linearize the system (1.1) to get the linear system (8.1). Diagonalize the system to arrive at

$$\frac{\partial W}{\partial t} + \Lambda(W_*)\frac{\partial W}{\partial x} = L(W_*)S(x, W_*) =: H(x, W_*), \tag{8.2}$$

where $W = L(U_*)U$, $L = (L_1, \cdots, L_m)^\top$, L_i is the left (row) eigenvector associated with λ_i, and Λ is a diagonal matrix with entries $\lambda_i(U_*)$. Therefore we can calculate the time derivative of W, as in the scalar case,

$$\left(\frac{\partial W}{\partial t}\right)_* = \lim_{t\to 0^+}\frac{\partial W}{\partial t}(0,t) = -\left[\frac{|\Lambda| + \Lambda}{2}W_L' + \frac{|\Lambda| - \Lambda}{2}W_R'\right] + H(x, W_*), \tag{8.3}$$

where $|\Lambda| = \mathrm{diag}(|\lambda_1|, \cdots, |\lambda_m|)$. This is an $O(\Delta t)$ approximation of the time derivatives appearing in (1.5). Returning to the original variables U we get

$$\left(\frac{\partial U}{\partial t}\right)_* = L^{-1}(U_*)\left(\frac{\partial W}{\partial t}\right)_*. \tag{8.4}$$

The resulting scheme is labelled as the G_1*–scheme.* In the original GRP scheme [4], there are the corresponding E_1 (Eulerian) scheme and L_1 (Lagrangian) scheme. Observe that when $U_L' = U_R' = 0$, the scheme degenerates to the Godunov scheme. Thus the G_1–scheme is the simplest possible extension of the Godunov scheme. Once the Godunov scheme is implemented, the implementation of the G_1–scheme adds a negligible amount of computational effort.

9. Several examples in applications

In this section we use the methodology developed above in order to treat several well-known physical examples. Our first two examples, the system of isentropic compressible fluid flow and the system of rotating shallow water equations, are endowed with coordinate systems of Riemann invariants so that they can be treated by the method of Sections 4–6. The third example, the system of nonisentropic compressible fluid flow in a duct of variable cross-section, does not possess a full coordinate system of Riemann invariants although there exist Riemann invariants for each characteristic field. However, this system falls into the category of weakly coupled systems, as defined in Definition 7.7.

9.1. **Isentropic compressible fluid flow.** The system of one-dimensional isentropic flow in gas dynamics is given by

$$\frac{\partial \rho}{\partial t} + \frac{\partial(\rho u)}{\partial x} = 0, \qquad \frac{\partial(\rho u)}{\partial t} + \frac{\partial(\rho u^2 + p(\rho))}{\partial x} = 0, \tag{9.1}$$

where $\rho \geq 0$ is the density, u is the velocity, and $p(\rho) = a\rho^\gamma$ is the pressure, $a > 0$ and $\gamma > 1$ are given constants. The system (9.1) has two eigenvalues

$$\lambda_- = u - c, \quad \lambda_+ = u + c, \tag{9.2}$$

where c is the speed of sound, given by $c^2 = a\gamma\rho^{\gamma-1}$. The two Riemann invariants are taken as

$$\phi = u - \frac{2c}{\gamma-1}, \qquad \psi = u + \frac{2c}{\gamma-1}, \tag{9.3}$$

where ϕ is associated with λ_+, and ψ is associated with λ_-. In terms of these Riemann invariants, the system (9.1) is reduced to a diagonal system (see (4.2))

$$\frac{\partial\phi}{\partial t} + \lambda_- \frac{\partial\phi}{\partial x} = 0, \qquad \frac{\partial\psi}{\partial t} + \lambda_+ \frac{\partial\psi}{\partial x} = 0. \tag{9.4}$$

We consider a typical local wave pattern consisting of a rarefaction wave moving to the left and a shock moving to the right, and assume that the t-axis is located inside the intermediate region, as in Figure 2.1. However, note that there is no contact discontinuity in the present case. In order to resolve the rarefaction wave, we need to set up the associated characteristic coordinates (α, β). Taking (α, β) as in Section 4, we obtain the following explicit expressions (cf. [5]),

$$t_{ass}(\alpha,\beta) = \frac{\alpha}{(\psi_L - \beta)^{\frac{1}{2\mu^2}}}, \qquad x_{ass}(\alpha,\beta) = \frac{\alpha\beta}{(\psi_L - \beta)^{\frac{1}{2\mu^2}}}, \quad \mu^2 = \frac{\gamma-1}{\gamma+1}. \tag{9.5}$$

The Hugoniot loci for shocks are given by

$$\sigma = \frac{\rho u - \overline{\rho u}}{\rho - \overline{\rho}}, \quad u = \overline{u} \pm \left(\frac{1}{\rho\overline{\rho}} \cdot (p(\rho) - p(\overline{\rho}))(\rho - \overline{\rho})\right)^{\frac{1}{2}} := \overline{u} \pm \Phi(\rho, \overline{\rho}), \tag{9.6}$$

where $\sigma(t) = x'(t)$ is the shock speed, $(\overline{\rho}, \overline{u})$ and (ρ, u) are the preshock and postshock states, respectively.

The following proposition is a straightforward application of Theorems 6.1 and 6.2.

Proposition 9.1. *Consider the system (9.1) subject to the piecewise initial data (2.1). Assume a typical wave pattern consisting of a rarefaction wave propagating to the left and a shock moving to the right. Then the limiting values $(\partial\rho/\partial t)_*$ and $(\partial u/\partial t)_*$ (see (2.2)) are determined by a pair of linear equations,*

$$\begin{aligned} a_L \left(\frac{\partial u}{\partial t}\right)_* + b_L \left(\frac{\partial \rho}{\partial t}\right)_* &= d_L, \\ a_R \left(\frac{\partial u}{\partial t}\right)_* + b_R \left(\frac{\partial \rho}{\partial t}\right)_* &= d_R. \end{aligned} \tag{9.7}$$

The coefficients a_L, b_L, d_L, a_R, b_R, d_R are given explicitly in the following two cases.

(i) **(Non-sonic case.)** *When the t-axis is located inside the intermediate region between the rarefaction wave and the shock, we have the non-sonic case,*

$$a_L = 1, \quad b_L = \frac{c_*}{\rho_*}, \quad d_L = -(u_* + c_*)\left(\frac{c_*}{c_L}\right)^{\frac{1}{2\mu^2}-1}\left(u_L' + \frac{c_L}{\rho_L}\rho_L'\right),$$

$$a_R = 1 - \frac{\sigma_0 u_*}{u_*^2 - c_*^2} - \frac{\partial\Phi}{\partial\rho}\cdot\frac{\sigma_0\rho_*}{u_*^2 - c_*^2}, \quad b_R = \frac{\sigma_0}{u_*^2 - c_*^2}\cdot\frac{c_*^2}{\rho_*} - \frac{\partial\Phi}{\partial\rho}\cdot\left(1 - \frac{\sigma_0 u_*}{u_*^2 - c_*^2}\right), \tag{9.8}$$

$$d_R = \frac{3(\sigma_0 - u_R)^2 + c_R^2}{2(\sigma_0 - u_R)}\cdot u_R' - \frac{(\sigma_0 - u_R)^2 + 3c_R^2}{2\rho_R}\rho_R',$$

and

$$\sigma_0 = \frac{\rho_* u_* - \rho_R u_R}{\rho_* - \rho_R}, \qquad \frac{\partial\Phi}{\partial\rho} = \frac{(\sigma_0 - u_*)^2 + c_*^2}{2\rho_*(\sigma_0 - u_*)}. \tag{9.9}$$

(ii) **(Sonic case.)** *When the t-axis (the cell interface) is located inside the rarefaction wave associated with λ_-, we have the sonic case. The coefficients a_L, b_L and d_L are given in (9.8) in which (ρ_*, u_*, c_*) is replaced by (ρ_0, u_0, c_0) there (such that $c_0 - u_0 = 0$, cf. Subsection 6.1), and a_R, b_R, d_R are given by*

$$a_R = 1.0, \qquad b_R = -\frac{c_0}{\rho_0}, \qquad d_R = 0.0. \tag{9.10}$$

9.2. **Rotating shallow water equations with Coriolis force.** We consider the shallow water motion on the rotating plane without dependence on one of the coordinates (say, y). This system was investigated in [6] and references therein. We use this system to illustrate the performance of our GRP scheme. The governing system can be written in the following form,

$$\frac{\partial h}{\partial t} + \frac{\partial(hu)}{\partial x} = 0,$$

$$\frac{\partial(hu)}{\partial t} + \frac{\partial(hu^2 + gh^2/2)}{\partial x} = fhv, \tag{9.11}$$

$$\frac{\partial(hv)}{\partial t} + \frac{\partial(huv)}{\partial x} = -fhu,$$

where h is the height of water, u, v are two components of the velocity, f is the (constant) Coriolis force coefficient, g is the gravitational constant. Note that the first two equations (with $f = 0$) are actually the one-dimensional shallow water model [13] and they are equivalent to the one-dimensional isentropic system (9.1), where h is regarded as ρ and $\gamma = 2$. A difference from (9.1) is the weak coupling with the other velocity component v through the source terms, while v is transported with the velocity u. Another difference is that there is a contact discontinuity associated with the eigenvalue u, across which h and u are continuous, and v has a jump.

The system (9.11) has the Riemann invariants v, and

$$\phi = u - 2c, \quad \psi = u + 2c, \tag{9.12}$$

where $c = \sqrt{gh}$. The pairs (v, ψ), (v, ϕ) and (ϕ, ψ) are, respectively, associated with the eigenvalues $\lambda_- = u - c$, $\lambda_+ = u + c$ and u. They comprise a coordinate system of Riemann invariants of the system (9.11). In terms of ϕ, ψ and v, we reduce (9.11) to the characteristic (diagonal) form,

$$\frac{\partial \phi}{\partial t} + \lambda_- \frac{\partial \phi}{\partial x} = fv, \quad \frac{\partial \psi}{\partial t} + \lambda_+ \frac{\partial \psi}{\partial x} = fv, \qquad \frac{\partial v}{\partial t} + u \frac{\partial v}{\partial x} = -fu. \tag{9.13}$$

Since the genuinely nonlinear eigenvalues $u - c$ and $u + c$ are the same as those for (9.1), we can use the same characteristic coordinates as in (9.5) when $\gamma = 2$. That is, throughout the rarefaction wave associated with $u - c$, the characteristic coordinates (α, β) are expressed as

$$t_{ass}(\alpha, \beta) = \frac{\alpha}{(\psi_L - \beta)^{\frac{3}{2}}}, \qquad x_{ass}(\alpha, \beta) = \frac{\alpha\beta}{(\psi_L - \beta)^{\frac{3}{2}}}. \tag{9.14}$$

In analogy with (9.1), we immediately have the limiting values $(\partial h/\partial t)_*$ and $(\partial u/\partial t)_*$. However, there is a small difference due to the presence of source terms in the current case. Also, we have the third wave (contact discontinuity) associated with u. As we see in the following propositions, this additional wave imposes no difficulty in the resolution of rarefaction waves and shocks.

Proposition 9.2. *Assume the configuration as shown in Figure 2.1, i.e, a rarefaction wave moves to the left and a shock moves to the right. Then we can apply the same approach as Proposition 9.1 in order to obtain the time derivatives $(\partial h/\partial t)_*$ and $(\partial u/\partial t)_*$ (replacing ρ by h and $\gamma = 2$). The coefficients a_L, b_L, a_R and b_R are given in (9.8), while d_L and d_R are given as follows.*

(i) For the non-sonic case, we have

$$\begin{aligned} d_L &= -(u_* + c_*) \cdot \left(\frac{c_*}{c_L}\right)^{\frac{1}{2}} \left(u_L' + \frac{c_L}{\rho_L}\rho_L'\right) + fv_L, \\ d_R &= \frac{3(\sigma_0 - u_R)^2 + c_R^2}{2(\sigma_0 - u_R)} \cdot u_R' - \frac{(\sigma_0 - u_R)^2 + 3c_R^2}{2\rho_R}\rho_R' \\ &\quad + fv_R \left[1 - \frac{\sigma_0}{u_*^2 - c_*^2} \cdot \frac{\sigma_0^2 - u_*^2 + c_*^2}{2(\sigma_0 - u_*)}\right]. \end{aligned} \tag{9.15}$$

(ii) For the sonic case, d_L is given in (9.15), and d_R is given as

$$d_R = fv_L. \tag{9.16}$$

Next we treat the variable v. Note that for the associated Riemann problem, $v = v_L$ across the rarefaction wave, and $v = v_R$ across the shock. For the case of the GRP (i.e., the initial data for v is piecewise linear), we have the following result for $(\partial v/\partial t)_*$.

Proposition 9.3. *Assume the configuration in Figure 2.1. Then we have:*
(i) if $u_* > 0$, the value $(\partial v/\partial t)_*$ is obtained from the rarefaction wave (left hand) side,

$$\left(\frac{\partial v}{\partial t}\right)_* = -Fr_* \left(\frac{c_*}{c_L}\right)^3 c_L v_L'$$

$$+fFr_* \left[-u_L + 3c_* \left(1 - \left(\frac{c_*}{c_L}\right)^2\right) - 2c_L \left(1 - \left(\frac{c_*}{c_L}\right)^3\right) + (u_* - c_*)\right], \tag{9.17}$$

where the Froude number $Fr_* = u_*/c_*$;
(ii) if $u_* < 0$, the value $(\partial v/\partial t)_*$ is calculated from the shock (right hand) side,

$$\left(\frac{\partial v}{\partial t}\right)_* = \frac{u_*(\sigma_0 - u_R)}{u_* - \sigma_0}\left[v_R' + f\right], \tag{9.18}$$

where σ_0 is the initial speed of the shock wave.

Proof. When $u_* > 0$, we see that v is continuous to the left of the contact discontinuity $\frac{dx}{dt} = u$. We can use the same method as in Theorems 4.3 and 4.4: Using the characteristic coordinates (α, β) and taking v as a Riemann invariant, we first calculate $\partial v/\partial\alpha(0, \beta)$ and then return to express the derivatives of v with respect to x and t, yielding (9.17).

When $u_* < 0$, we use the continuity property of v across the shock and differentiate along the shock trajectory $x = x(t)$ to get

$$\frac{\partial v(x(t) - 0, t)}{\partial t} + \sigma(t)\frac{\partial v(x(t) - 0, t)}{\partial x} = \frac{\partial v(x(t) + 0, t)}{\partial t} + \sigma(t)\frac{\partial v(x(t) + 0, t)}{\partial x}, \tag{9.19}$$

where $\sigma(t)$ is the shock speed. Using the equation for v in (9.13), substituting the spatial derivative of v in the postshock side by the time derivative and the time derivative in the preshock side by the spatial derivative, we then take the limit to obtain (9.18). □

9.3. **A variable area duct flow.** We now consider the variable area duct flow governed by the system [4, Chapter 4]

$$\frac{\partial(A(x)\rho)}{\partial t} + \frac{\partial(A(x)\rho u)}{\partial x} = 0,$$

$$\frac{\partial(A(x)\rho u)}{\partial t} + \frac{\partial(A(x)\rho u^2)}{\partial x} + A(x)\frac{\partial p}{\partial x} = 0, \tag{9.20}$$

$$\frac{\partial(A(x)\rho E)}{\partial t} + \frac{\partial(A(x)u(\rho E + p))}{\partial x} = 0,$$

where the variables ρ, u, p and E are the density, velocity, pressure and the total specific energy. The total specific energy consists of two parts $E = \frac{u^2}{2} + e$, e is the internal specific energy. The function $A(x)$ is the area of the duct. When $A(x) \equiv 1$, the system (9.20) represents the planar compressible Euler equations. Let T be the temperature. Then the entropy S can be defined, as usual, by the second law of thermodynamics,

$$TdS = de - \frac{p}{\rho^2}d\rho. \tag{9.21}$$

In terms of ρ, u and S, the system (9.20) can be written, for smooth flows, as,

$$\frac{\partial \rho}{\partial t} + u\frac{\partial \rho}{\partial x} + \rho\frac{\partial u}{\partial x} = -\frac{A'(x)}{A(x)}\rho u,$$

$$\frac{\partial u}{\partial t} + u\frac{\partial u}{\partial x} + \frac{1}{\rho}\frac{\partial p}{\partial x} = 0, \tag{9.22}$$

$$\frac{\partial S}{\partial t} + u\frac{\partial S}{\partial x} = 0,$$

where p is regarded as a function of ρ and S. We discuss the case of polytropic gases, for which the internal energy $e = \frac{p}{(\gamma-1)\rho}$. Then in terms of ρ, u and p, the third equation of (9.22) can be replaced by,

$$\frac{\partial p}{\partial t} + u\frac{\partial p}{\partial x} + \rho c^2\frac{\partial u}{\partial x} = -\frac{A'(x)}{A(x)}\rho c^2 u. \tag{9.23}$$

Here c is the local speed of sound, given by $c^2 = \frac{\gamma p}{\rho}$. Note that (9.22) is just valid for smooth flows. For non-smooth flows, we need to use the conservative form (9.20) with the conserved variables $(\rho, \rho u, \rho E)$.

The system (9.20), or equivalently (9.22), possesses three eigenvalues

$$\lambda_- = u - c, \quad \lambda_0 = u, \quad \lambda_+ = u + c. \tag{9.24}$$

We introduce two variables ϕ, ψ [5],

$$\phi = u - \int^\rho \frac{c(\omega, S)}{\omega}d\omega, \qquad \psi = u + \int^\rho \frac{c(\omega, S)}{\omega}d\omega. \tag{9.25}$$

The functions ϕ, ψ can be expressed in terms of total differentials, see [5, Eqs. (2.6), (2.10) and (2.15)]

$$d\phi = du - \frac{1}{\rho c}dp - \frac{T}{c}dS, \quad d\psi = du + \frac{1}{\rho c}dp + \frac{T}{c}dS. \tag{9.26}$$

For the entropy S, we have

$$TdS = \frac{dp}{(\gamma-1)\rho} - \frac{c^2}{(\gamma-1)\rho}d\rho. \tag{9.27}$$

The three pairs (ψ, S), (u, p) and (ϕ, S) are the Riemann invariants associated with λ_-, λ_0 and λ_+, respectively. However, there is no full coordinate system of Riemann invariants so that (9.20) cannot be reduced to a diagonal form. At this point, the system (9.20) is substantially different from the system of isentropic flow (9.1) and the system of shallow water equations (9.11). However, it falls into the category of weakly coupled systems, as defined in Definition 7.7. Indeed, we take ϕ, ψ and S as the (quasi)-Riemann invariants to

write (9.22) as

$$\begin{cases} \dfrac{\partial \phi}{\partial t} + (u-c)\dfrac{\partial \phi}{\partial x} = B_1, \\ \dfrac{\partial \psi}{\partial t} + (u+c)\dfrac{\partial \psi}{\partial x} = B_2, \\ \dfrac{\partial S}{\partial t} + u\dfrac{\partial S}{\partial x} = 0. \end{cases} \tag{9.28}$$

where $B_1 = T\frac{\partial S}{\partial x} + \frac{A'(x)}{A(x)}cu$, $B_2 = T\frac{\partial S}{\partial x} - \frac{A'(x)}{A(x)}cu$. For the present system, $W^a = (\phi, \psi)^\top$ and $W^b = S$, corresponding to Definition 7.7.

We use this weakly coupled form to resolve the generalized Riemann problem for (9.20) subject to piecewise linear initial data of the form (2.1). Assume that the configuration is as shown in Figure 2.1; a rarefaction wave associated with $u - c$ moves to the left, a shock associated with $u + c$ moves to the right, and the t-axis is located inside the intermediate region. Denote by p_*, u_* the limiting values of p, u at the contact discontinuity as $t \to 0_+$. Similarly, denote by ρ_{*1}, c_{*1} and ρ_{*2}, c_{*2} the limiting values of ρ, c on the left-hand and right-hand sides of the contact discontinuity, respectively. Then we resolve the rarefaction wave, the shock and the contact discontinuity, separately.

First we resolve the rarefaction wave associated with $u-c$ from the left. According to the general treatment of weakly coupled system in Section 7, this is done by first treating W^b and solving for W^a. In our case, it means that we are using the Riemann invariants ϕ, ψ with appropriate dependence on S. Due to the special form of the system, the dependence of S is very simple. For this purpose, we need to establish the system of characteristic coordinates $(x,t) \to (\alpha, \beta)$, where α and β are defined in terms of the eigenvalues $u + c$, $u-c$, respectively. See Figure 2.1 and the section of Figure 4.1. The associated characteristic coordinates $t_{ass}(\alpha,\beta)$, $x_{ass}(\alpha,\beta)$ are given in (9.5). In the limit $\alpha \to 0$, $u(0,\beta) - c(0,\beta) = \beta$ so that $c = \mu^2(\psi_L - \beta)$ and $u = (\mu^2 - 1)(\psi_L - \beta) + \psi_L$, where $\mu^2 = \frac{\gamma-1}{\gamma+1}$, $\psi_L = \psi(\rho_L, u_L, p_L)$. Eqs. (9.4) are replaced by the first two equations of (9.28). According to Theorem 7.3, we obtain $\partial\psi/\partial t$ and $\partial S/\partial t$, as stated in the following proposition.

Proposition 9.4. *Assume that the rarefaction wave associated with $u-c$ moves to the left, as in Figure 2.1. Consider the Riemann invariants S, ψ and their time derivatives $\partial S/\partial t$, $\partial\psi/\partial t$ as continuous functions of α, β, in the rectangle $-\alpha_0 \le \alpha \le 0$, $\beta_L \le \beta \le \beta_*$ for some $\alpha_0 > 0$. Then we have,*

$$\begin{aligned} &T\frac{\partial S}{\partial t}(0,\beta) = -(\beta + c_L\theta)\theta^{\frac{2\gamma}{\gamma-1}}T_L S_L', \qquad \theta = c(0,\beta)/c_L, \\ &\frac{\partial \psi}{\partial t}(0,\beta) = H_1 + \frac{A'(0)}{2A(0)}H_2, \end{aligned} \tag{9.29}$$

where $T_L S_L'$ is defined by (9.27), and H_1, H_2 are given by,

$$H_1 = -\frac{\beta + c_L\theta}{c_L}\theta^{\frac{\gamma+1}{\gamma-1}} T_L S_L' + \frac{\beta + 2c_L\theta}{c_L}\theta^{\frac{3-\gamma}{2(\gamma-1)}}\left[\frac{2\gamma}{3\gamma-1} T_L S_L' - c_L\psi_L'\right],$$

$$H_2 = \beta(\beta + c_L\theta) - (\beta + 2c_L\theta)\left[u_L\theta^{\frac{3-\gamma}{2(\gamma-1)}} + \overline{H_2}\right],$$

(9.30)

$$\overline{H_2} = \begin{cases} \dfrac{-2(\gamma+1)c_L\theta}{(\gamma-1)(3\gamma-5)}\left(1-\theta^{\frac{5-3\gamma}{2(\gamma-1)}}\right) - \dfrac{(\gamma+1)\psi_L}{\gamma-3}\left[1-\theta^{\frac{3-\gamma}{2(\gamma-1)}}\right], & \text{if } \gamma \neq 3, 5/3, \\ 2c_L(\theta-1) - \psi_L\ln\theta, & \text{if } \gamma = 3, \\ 2\left[c_L\theta\ln\theta + \psi_L(1-\theta)\right], & \text{if } \gamma = 5/3. \end{cases}$$

Proof. According to the general treatment of Section 7, we need to consider the evolution of the time derivatives of two pairs of Riemann invariants (ϕ, S) and (ϕ, ψ).

(i) The computation of $T\partial S/\partial t$. we use the first and third equations of (9.28) to form a system of two equations,

$$\begin{cases} \dfrac{\partial\phi}{\partial t} + (u-c)\dfrac{\partial\phi}{\partial x} = B_1, \\ \dfrac{\partial S}{\partial t} + (u+c)\dfrac{\partial S}{\partial x} = c\dfrac{\partial S}{\partial x}. \end{cases} \tag{9.31}$$

Then, in terms of α and β, we have (since $\partial x/\partial\alpha = (u-c)\partial t/\partial\alpha$ and $\partial x/\partial\beta = (u+c)\partial t/\partial\beta$),

$$\begin{aligned} \frac{\partial S}{\partial\beta} &= \frac{\partial t}{\partial\beta}\cdot\left[\frac{\partial S}{\partial t} + (u+c)\frac{\partial S}{\partial x}\right] = \frac{\partial t}{\partial\beta}\cdot c\frac{\partial S}{\partial x}, \\ \frac{\partial S}{\partial\alpha} &= \frac{\partial t}{\partial\alpha}\left[\frac{\partial S}{\partial t} + (u-c)\frac{\partial S}{\partial x}\right] = -\frac{\partial t}{\partial\alpha}\cdot c\frac{\partial S}{\partial x}. \end{aligned} \tag{9.32}$$

We note, as in (4.15), that

$$\frac{\partial^2 t}{\partial\alpha\partial\beta}(0,\beta) = \frac{1}{2c(0,\beta)}\frac{\partial t}{\partial\alpha}(0,\beta), \tag{9.33}$$

where we have used the fact that $\lambda_-(0,\beta) = \beta$, $\lambda_-(0,\beta) - \lambda_+(0,\beta) = -2c(0,\beta)$ and $(\partial t/\partial\beta)(0,\beta) = 0$. Thus, differentiating the first equation of (9.32) with respect to α and noting $\frac{\partial t}{\partial\beta}(0,\beta) \equiv 0$, we get

$$\frac{\partial}{\partial\beta}\left(\frac{\partial S}{\partial\alpha}(0,\beta)\right) = \frac{1}{2}\frac{\partial t}{\partial\alpha}(0,\beta)\cdot\frac{\partial S}{\partial x}(0,\beta) = -\frac{1}{2c(0,\beta)}\frac{\partial S}{\partial\alpha}(0,\beta). \tag{9.34}$$

Integrating from β_L to β yields,

$$\frac{\partial S}{\partial\alpha}(0,\beta) = \frac{\partial S}{\partial\alpha}(0,\beta_L)\exp\left(-\int_{\beta_L}^{\beta}\frac{1}{2c(0,\eta)}d\eta\right) = \frac{\partial S}{\partial\alpha}(0,\beta_L)\cdot\theta^{\frac{1}{2\mu^2}}. \tag{9.35}$$

Similarly, we get from (9.33)

$$\frac{\partial t}{\partial \alpha}(0,\beta) = \frac{\partial t}{\partial \alpha}(0,\beta_L)\theta^{-\frac{1}{2\mu^2}}. \tag{9.36}$$

In particular, from the second equation of (9.32) and(9.36), we have

$$c(0,\beta)\frac{\partial S}{\partial x}(0,\beta) = -\frac{\partial S}{\partial \alpha}(0,\beta)\cdot\left(\frac{\partial t}{\partial \alpha}\right)^{-1}(0,\beta) = c_L S_L'\theta^{\frac{1}{\mu^2}}. \tag{9.37}$$

Hence using the entropy equation in (9.28), we return to the (x,t)-coordinate system to get $T\frac{\partial S}{\partial t}$,

$$T(0,\beta)\frac{\partial S}{\partial t}(0,\beta) \ = -u(0,\beta)T(0,\beta)\frac{\partial S}{\partial x}(0,\beta), \tag{9.38}$$

which gives $T\frac{\partial S}{\partial t}$ in (9.29) by using (9.37) and noting $T/T_L = c^2/c_L^2$.

(ii) The computation of $\partial\psi/\partial t$. We now consider the first two equations in (9.28), i.e., the system of two equations,

$$\begin{cases} \dfrac{\partial \phi}{\partial t} + (u-c)\dfrac{\partial \phi}{\partial x} = B_1, \\[2ex] \dfrac{\partial \psi}{\partial t} + (u+c)\dfrac{\partial \psi}{\partial x} = B_2. \end{cases} \tag{9.39}$$

As in (9.32), we note

$$\frac{\partial \psi}{\partial t} + (u-c)\frac{\partial \psi}{\partial x} = \left(\frac{\partial t}{\partial \alpha}\right)^{-1}\frac{\partial \psi}{\partial \alpha}. \tag{9.40}$$

Regard the source terms as functions of (α,β). In the limit $(\alpha \to 0)$, they are known from the first part of the proof, see Eq. (9.37). In terms of the general treatment of weakly coupled systems in Section 7, this is at the stage where W^b $(= \{S\})$ is fully resolved, and we can turn to the diagonal system for W^a $(= \{\phi,\psi\})$. Following the same reasoning as the one leading up to equation (9.34), we get

$$\frac{\partial}{\partial \beta}\left(\frac{\partial \psi}{\partial \alpha}(0,\beta)\right) = \frac{1}{2c(0,\beta)}\cdot\frac{\partial t}{\partial \alpha}(0,\beta)\cdot B_2(0,\beta). \tag{9.41}$$

The integration from β_L to β yields,

$$\frac{\partial \psi}{\partial \alpha}(0,\beta) = \frac{\partial \psi}{\partial \alpha}(0,\beta_L) + \int_{\beta_L}^{\beta}\frac{1}{2c(0,\eta)}\cdot\frac{\partial t}{\partial \alpha}(0,\eta)\cdot B_2(0,\eta)d\eta, \tag{9.42}$$

The initial data for $\partial\psi/\partial\alpha$ is given by

$$\frac{\partial \psi}{\partial \alpha}(0,\beta_L) = \frac{\partial t}{\partial \alpha}(0,\beta_L)\left[T_L S_L' - \frac{A'(0)}{A(0)}c_L u_L - 2c_L\psi_L'\right], \tag{9.43}$$

where we note the following relation by using (9.39) and (9.40),

$$\frac{\partial \psi}{\partial \alpha} = \frac{\partial t}{\partial \alpha}\cdot\left[\frac{\partial \psi}{\partial t} + (u-c)\frac{\partial \psi}{\partial x}\right] = \frac{\partial t}{\partial \alpha}\cdot\left[B_2 - 2c\frac{\partial \psi}{\partial x}\right]. \tag{9.44}$$

Once we obtain $(\partial\psi/\partial\alpha)(0,\beta)$ from (9.42), we get

$$2c(0,\beta)\frac{\partial\psi}{\partial x}(0,\beta) = B_2(0,\beta) - \left(\frac{\partial t}{\partial\alpha}\right)^{-1}(0,\beta)\frac{\partial\psi}{\partial\alpha}(0,\beta). \tag{9.45}$$

we insert this into (9.40) to get

$$\frac{\partial\psi}{\partial t}(0,\beta) = -\frac{u-c}{2c}B_2(0,\beta) + \frac{u+c}{2c}\left(\frac{\partial t}{\partial\alpha}\right)^{-1}\frac{\partial\psi}{\partial\alpha}(0,\beta). \tag{9.46}$$

Then using $B_2(0,\beta) = T(0,\beta)\frac{\partial S}{\partial x}(0,\beta) - \frac{A'(0)}{A(0)}c(0,\beta)u(0,\beta)$ and the value $\frac{\partial\psi}{\partial\alpha}(0,\beta)$ in (9.42), we obtain the second equation in (9.29). □

Proposition 9.5. *(Resolution of rarefaction waves.) Assume that the rarefaction wave associated with $u-c$ moves to the left. Use the characteristic coordinates (α,β) as above and consider the limiting values $\frac{\partial u}{\partial t}(0,\beta)$ and $\frac{\partial p}{\partial t}(0,\beta)$, $\beta_L \le \beta \le \beta_*$. Then we have*

$$\tilde{a}_L(0,\beta)\frac{\partial u}{\partial t}(0,\beta) + \tilde{b}_L(0,\beta)\frac{\partial p}{\partial t}(0,\beta) = \tilde{d}_L(\beta), \tag{9.47}$$

where the coefficients $\tilde{a}_L$, $\tilde{b}_L$ and $\tilde{d}_L$ can be expressed explicitly as follows. With $\theta = c(0,\beta)/c_L$,

$$\tilde{a}_L(0,\beta) = 1, \quad \tilde{b}_L(0,\beta) = \frac{1}{\rho(0,\beta)c(0,\beta)}, \tag{9.48}$$

and

$$\tilde{d}_L(\beta) = \frac{\beta + 2\theta c_L}{c_L}\cdot\theta^{\frac{3-\gamma}{2(\gamma-1)}}\left(\frac{2\gamma}{3\gamma-1}T_L S_L' - c_L\psi_L'\right) + \frac{A'(0)}{2A(0)}H_2, \tag{9.49}$$

where H_2 is given in (9.30).

Proof. We use (9.26) to get

$$\frac{\partial u}{\partial t} + \frac{1}{\rho c}\frac{\partial p}{\partial t} = \frac{\partial\psi}{\partial t} - \frac{T}{c}\frac{\partial S}{\partial t}. \tag{9.50}$$

The right-hand side can be evaluated at $(0,\beta)$ using the two equations in (9.29) to yield (9.47) as well.

□

As in Section 7.3, we can use the Riemann invariants W for the resolution of jump discontinuities. However, as in the first part of Section 7.3, it is more convenient to use the basic primitive variables $U = (\rho, u, p)$. See Remark 7.11.

The Rankine-Hugoniot conditions for shocks are

$$\sigma = \frac{\rho u - \overline{\rho u}}{\rho - \overline{\rho}}, \quad u = \overline{u} \pm \Phi(p;\overline{p},\overline{\rho}), \qquad \rho = h(p;\overline{p},\overline{\rho}), \tag{9.51}$$

where (ρ,u,p) and $(\overline{\rho},\overline{u},\overline{p})$ are the states ahead and behind the shock, respectively, and

$$\Phi(p;\overline{p},\overline{\rho}) = (p-\overline{p})\sqrt{\frac{1-\mu^2}{\overline{\rho}(p+\mu^2\overline{p})}}, \qquad h(p;\overline{p},\overline{\rho}) = \overline{\rho}\frac{p+\mu^2\overline{p}}{\overline{p}+\mu^2 p}, \quad \mu^2 = \frac{\gamma-1}{\gamma+1}. \tag{9.52}$$

Assume that this shock is associated with $u+c$ and moves to the right, as shown in Figure 2.1. Then it can be resolved with a standard method, see [5].

Proposition 9.6. *(Resolution of shocks.) Assume that a shock associated with $u+c$ moves to the right. Then the limiting values $(\partial p/\partial t)_*$ and $(\partial u/\partial t)_*$ satisfy the linear relations*

$$\tilde{a}_R \left(\frac{\partial u}{\partial t}\right)_* + \tilde{b}_R \left(\frac{\partial p}{\partial t}\right)_* = \tilde{d}_R, \tag{9.53}$$

where the coefficients are given explicitly in the following,

$$\begin{aligned}
&\tilde{a}_R = 1 - \frac{\sigma_0 u_*}{u_*^2 - c_{*2}^2} - \frac{\sigma_0 \rho_{*2} c_{*2}^2}{u_*^2 - c_{*2}^2}\cdot \Phi_1, \quad \tilde{b}_R = \frac{1}{\rho_{*2}}\frac{\sigma_0}{u_*^2 - c_{*2}^2} - \left(1 - \frac{\sigma_0 u_*}{u_*^2 - c_{*2}^2}\right)\Phi_1,\\
&\tilde{d}_R = L_p^R \cdot p_R' + L_u^R \cdot u_R' + L_\rho^R \cdot \rho_R' + \frac{A'(0)}{A(0)} j_R,
\end{aligned} \tag{9.54}$$

and

$$\begin{aligned}
L_p^R &= -\frac{1}{\rho_R} + (\sigma_0 - u_R)\cdot \Phi_2,\\
L_u^R &= \sigma_0 - u_R - \rho_R \cdot c_R^2 \cdot \Phi_2 - \rho_R \cdot \Phi_3,\\
L_\rho^R &= (\sigma_0 - u_R)\cdot \Phi_3,\\
j_R &= -(\Phi_2 c_{*2}^2 + \Phi_3)\rho_R u_R + (1 + \Phi_1 \rho_{*2} u_*)\,\frac{\sigma_0 c_{*2}^2 u_*}{u_*^2 - c_{*2}^2};
\end{aligned}$$

$$\begin{aligned}
\sigma_0 &= \frac{\rho_{*2} u_* - \rho_R u_R}{\rho_{*2} - \rho_R},\\
\Phi_1 &= \frac{1}{2}\sqrt{\frac{1-\mu^2}{\rho_R(p_* + \mu^2 p_R)}}\cdot \frac{p_* + (1+2\mu^2)p_R}{p_* + \mu^2 p_R},\\
\Phi_2 &= -\frac{1}{2}\sqrt{\frac{1-\mu^2}{\rho_R(p_* + \mu^2 p_R)}}\cdot \frac{(2+\mu^2)p_* + \mu^2 p_R}{p_* + \mu^2 p_R},\\
\Phi_3 &= -\frac{p_* - p_R}{2\rho_R}\sqrt{\frac{1-\mu^2}{\rho_R(p_* + \mu^2 p_R)}}.
\end{aligned} \tag{9.55}$$

Next we want to resolve the contact discontinuities. Let $x = x(t)$ be the jump discontinuity. The Rankine-Hugoniot (jump) conditions are

$$u(x(t)-0,t) = u(x(t)+0,t), \quad p(x(t)-0,t) = p(x(t)+0,t). \tag{9.56}$$

Indeed, u and p are the Riemann invariants associated with $\lambda_0 = u$. Denote $D/Dt = \partial/\partial t + u\partial/\partial x$, $u^\pm(t) := u(x(t)\pm 0, t)$, $p^\pm(t) = p(x(t)\pm 0, t)$. Then along $x = x(t)$ we have

$$\frac{Du^+(t)}{Dt} = \frac{Du^-(t)}{Dt}, \quad \frac{Dp^+(t)}{Dt} = \frac{Dp^-(t)}{Dt}. \tag{9.57}$$

Note that

$$\begin{aligned}\frac{\partial u}{\partial t} &= \frac{Du}{Dt} + \frac{u}{\rho c^2}\frac{Dp}{Dt} + \frac{A'(x)}{A(x)}u^2,\\ \frac{\partial p}{\partial t} &= \frac{Dp}{Dt} + \rho u\frac{Du}{Dt}.\end{aligned} \tag{9.58}$$

or

$$\begin{aligned}\frac{Du}{Dt} &= \frac{1}{c^2-u^2}\left[c^2\frac{\partial u}{\partial t} - \frac{u}{\rho}\frac{\partial p}{\partial t} - \frac{A'(x)}{A(x)}c^2u^2\right],\\ \frac{Dp}{Dt} &= \frac{c^2}{u^2-c^2}\left[\rho u\frac{\partial u}{\partial t} - \frac{\partial p}{\partial t} - \frac{A'(x)}{A(x)}\rho u^3\right].\end{aligned} \tag{9.59}$$

Then, once the limiting values $(\partial u/\partial t)_*$ and $(\partial p/\partial t)_*$ on one side of the contact discontinuity are known, then we can obtain them on the other side. We remind that they are different on the two sides since the density ρ experiences a jump there.

Combining all above discussion, we can solve the generalized Riemann problem (9.20) and (2.1). We summarize our results in the following propositions.

Proposition 9.7. *(Non-sonic case.) Assume a typical wave configuration for the generalized Riemann problem for (9.20) as shown in Figure 2.1. Then we can obtain $(\partial u/\partial t)_*$ and $(\partial p/\partial t)_*$ by solving the following pair of linear equations,*

$$\begin{aligned}a_L\left(\frac{\partial u}{\partial t}\right)_* + b_L\left(\frac{\partial p}{\partial t}\right)_* &= d_L,\\ a_R\left(\frac{\partial u}{\partial t}\right)_* + b_R\left(\frac{\partial p}{\partial t}\right)_* &= d_R,\end{aligned} \tag{9.60}$$

where a_L, b_L, d_L and a_R, b_R, d_R are specified below. Also the computation of $(\partial\rho/\partial t)_*$ are also computed by the following two cases.

(i) If $u_* > 0$, the contact discontinuity moves to the right. The coefficients a_L, b_L and d_L are given in (9.47),

$$(a_L, b_L, d_L) = (\tilde{a}_L, \tilde{b}_L, \tilde{d}_L). \tag{9.61}$$

The coefficients a_R, b_R and d_R are given by

$$\begin{aligned}a_R &= \frac{c_{*1}^2}{c_{*1}^2-u_*^2}\left[\tilde{a}_R(1-\frac{\rho_{*1}u_*^2}{\rho_{*2}c_{*2}^2}) + \tilde{b}_R(\rho_{*2}-\rho_{*1})u_*\right],\\ b_R &= \frac{1}{c_{*1}^2-u_*^2}\left[\tilde{a}_R(-\frac{1}{\rho_{*1}} + \frac{c_{*1}^2}{\rho_{*2}c_{*2}^2})u_* - \tilde{b}_R(-\frac{\rho_{*2}}{\rho_{*1}}u_*^2 + c_{*1}^2)\right],\\ d_R &= \tilde{d}_R + \frac{A'(0)}{A(0)}\frac{u_*^3}{c_{*1}^2-u_*^2}\left[\tilde{a}_R(1-\frac{\rho_{*1}c_{*1}^2}{\rho_{*2}c_{*2}^2}) + \tilde{b}_R(\rho_{*2}-\rho_{*1})c_{*1}^2\right].\end{aligned} \tag{9.62}$$

The value $(\partial\rho/\partial t)_*$ is computed from the rarefaction side,

$$\left(\frac{\partial\rho}{\partial t}\right)_* = \frac{1}{c_*^2}\left[\left(\frac{\partial p}{\partial t}\right)_* + (\gamma-1)\rho_* u_*\left(\frac{c_*}{c_L}\right)^{\frac{1+\mu^2}{\mu^2}} T_L S_L'\right], \tag{9.63}$$

by using the state equation $p = p(\rho, S)$.

(ii) If $u_* < 0$, *the contact discontinuity moves to the left. The coefficients* a_R, b_R *and* d_R *are given in Proposition 9.6,*

$$(a_R, b_R, d_R) = (\tilde{a}_R, \tilde{b}_R, \tilde{d}_R). \tag{9.64}$$

While the coefficients a_L, b_L *and* d_L *are computed by*

$$a_L = \frac{c_{*2}^2}{c_{*2}^2 - u_*^2}\left[\tilde{a}_L(1 - \frac{\rho_{*2}u_*^2}{\rho_{*1}c_{*1}^2}) + \tilde{b}_L(\rho_{*1} - \rho_{*2})u_*\right],$$

$$b_L = \frac{1}{c_{*2}^2 - u_*^2}\left[\tilde{a}_L(-\frac{1}{\rho_{*2}} + \frac{c_{*2}^2}{\rho_{*1}c_{*1}^2})u_* - \tilde{b}_L(-\frac{\rho_{*1}}{\rho_{*2}}u_*^2 + c_{*2}^2)\right], \tag{9.65}$$

$$d_L = \tilde{d}_L + \frac{A'(0)}{A(0)}\frac{u_*^3}{c_{*2}^2 - u_*^2}\left[\tilde{a}_L(1 - \frac{\rho_{*2}c_{*2}^2}{\rho_{*1}c_{*1}^2}) + \tilde{b}_L(\rho_{*1} - \rho_{*2})c_{*2}^2\right].$$

The value $(\partial\rho/\partial t)_*$ *is computed from the shock side,*

$$g_\rho^R\left(\frac{\partial\rho}{\partial t}\right)_* + g_p^R\left(\frac{Dp}{Dt}\right)_* + g_u^R\left(\frac{Du}{Dt}\right)_* = u_* \cdot f_R, \tag{9.66}$$

where g_ρ^R, g_p^R, g_u^R *and* f_R *are constant, explicitly given in the following,*

$$g_\rho^R = u_* - \sigma_0, \quad g_p^R = \frac{\sigma_0}{c_{*2}^2} - u_*H_1, \quad g_u^R = \rho_{2*}(\sigma_0 - u_*) \cdot u_* \cdot H_1,$$

$$\begin{aligned} f_R = \ & (\sigma_0 - u_R) \cdot H_2 \cdot p_R' + (\sigma_0 - u_R) \cdot H_3 \cdot \rho_R' - \rho_R \cdot (H_2c_R^2 + H_3) \cdot u_R' \\ & -\frac{A'(0)}{A(0)} \cdot \left(H_2c_R^2 + H_3\right)\rho_R u_R, \end{aligned} \tag{9.67}$$

and H_1, H_2 *and* H_3 *are expressed by*

$$H_1 = \frac{\rho_R(1-\mu^4)p_R}{(p_R + \mu^2 p_*)^2}, \quad H_2 = \frac{\rho_R(\mu^4 - 1)p_*}{(p_R + \mu^2 p_*)^2}, \quad H_3 = \frac{p_* + \mu^2 p_R}{p_R + \mu^2 p_*}. \tag{9.68}$$

Proposition 9.8. *(Sonic case). Assume that the* $t-$*axis is located inside the rarefaction wave associated with* $u - c$. *Then we have*

$$\left(\frac{\partial u}{\partial t}\right)_0 = \frac{1}{2}\left[\tilde{d}_L + \theta^{\frac{2\gamma}{\gamma-1}}T_L S_L' + \frac{A'(0)}{A(0)}u_0^2\right], \quad \left(\frac{\partial p}{\partial t}\right)_0 = \frac{\rho_0 c_0}{2}\left[\tilde{d}_L - \theta^{\frac{2\gamma}{\gamma-1}}T_L S_L' - \frac{A'(0)}{A(0)}u_0^2\right], \tag{9.69}$$

where $\tilde{d}_L$ *is given in (9.49), with* $\theta = c_0/c_L$, *and* (u_0, ρ_0, c_0) *is the limiting value of* (u, ρ, c) *along the* t*-axis so that* $u_0 - c_0 = 0$, *cf. the sonic case in Proposition 9.1.*

Proof. Note that at the origin, we have

$$\left(\frac{\partial\phi}{\partial t}\right)_0 = \left(\frac{\partial\phi}{\partial t}\right)_0 + (u_0 - c_0)\left(\frac{\partial\phi}{\partial x}\right)_0 = \left(T\frac{\partial S}{\partial x}\right)_0 + \frac{A'(0)}{A(0)}c_0u_0. \tag{9.70}$$

That is,

$$\left(\frac{\partial u}{\partial t}\right)_0 - \frac{1}{\rho_0 u_0}\left(\frac{\partial p}{\partial t}\right)_0 = \left(T\frac{\partial S}{\partial x}\right)_0 + \frac{A'(0)}{A(0)}c_0 u_0. \tag{9.71}$$

Since $(T\partial S/\partial x)_0 = \theta^{\frac{2\gamma}{\gamma-1}} T_L S'_L$, we use Proposition 9.5 to complete the proof. □

Finally we present the acoustic case that $U_L = U_R$ but $U'_L \neq U'_R$, which leads to the G_1 scheme.

Proposition 9.9. *(Acoustic case.) Assume that $U_L = U_R$ and $U'_L \neq U'_R$. Then we have the acoustic case, and $(\partial u/\partial t)_*$ and $(\partial p/\partial t)_*$ are solved as*

(9.72)

$$\left(\frac{\partial u}{\partial t}\right)_* = -\frac{1}{2}\left[(u_* + c_*)\left(u'_L + \frac{p'_L}{\rho_* c_*}\right) + (u_* - c_*)\left(u'_R - \frac{p'_R}{\rho_* c_*}\right)\right],$$

$$\left(\frac{\partial p}{\partial t}\right)_* = -\frac{\rho_* c_*}{2}\left[(u_* + c_*)\left(u'_L + \frac{p'_L}{\rho_* c_*}\right) - (u_* - c_*)\left(u'_R - \frac{p'_R}{\rho_* c_*}\right)\right] - \frac{A'(0)}{A(0)}\rho_* c_*^2 u_*.$$

The quantity $(\partial\rho/\partial t)_*$ is solved according to the direction of the contact discontinuity,

$$\left(\frac{\partial \rho}{\partial t}\right)_* = \frac{1}{c_*^2}\left[\left(\frac{\partial p}{\partial t}\right)_* + u_*\left(p'_L - c_*^2\rho'_L\right)\right] \tag{9.73}$$

if $u_* = u_L = u_R > 0$; and

$$\left(\frac{\partial \rho}{\partial t}\right)_* = \frac{1}{c_*^2}\left[\left(\frac{\partial p}{\partial t}\right)_* + u_*\left(p'_R - c_*^2\rho'_R\right)\right] \tag{9.74}$$

if $u_* = u_L = u_R < 0$.

10. Numerical Examples

In consistent with Section 9, we present several numerical examples to show the performance of our GRP scheme.

10.1. **The Riemann problem for isentropic flows.** Two examples are given for isentropic flows (9.1), see Figure 10.1, in which fifty grid points are used both for the Godunov scheme and the GRP scheme. The first simulates the dam collapse problem with an almost dry bed on one side. We clearly see that the sonic point glitch in the first order Gudonov solution is eliminated by the GRP scheme. Also this example shows that our GRP can preserve the positivity of the height of water. The second is the standard Riemann problem. The solution contains a shock propagating to the left and a rarefaction wave moving to the right. We see the high accuracy of the GRP scheme, particularly for the rarefaction wave, which may be due to its analytic resolution in our GRP scheme. Recall that in [12] the rarefactive wave is replaced by a rarefaction shock.

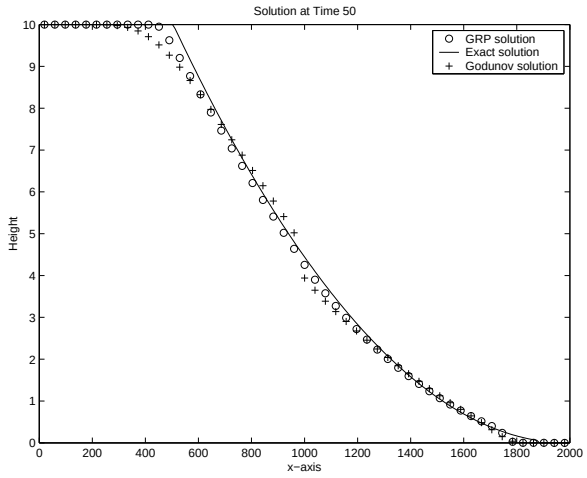

(a) Dam collapse problem with low height of water: $a = 4.9$, $\gamma = 2$

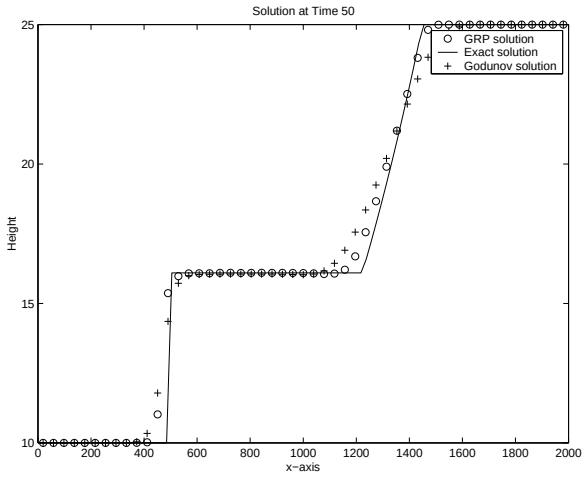

(b) Riemann problem for isentropic flow: $a = 1$, $\gamma = 1.4$

FIGURE 10.1. Numerical solutions for isentropic flows. (a). The Riemann initial data are: $\rho_L = 10.0$, $u_L = 0.0$, $\rho_R = 10^{-5}$, $u_R = 0.0$. (b). The Riemann initial data are: $\rho_L = 10.0$, $u_L = 0.0$, $\rho_R = 25$, $u_R = 0.0$.

10.2. **Rotating shallow water equations with Coriolis force.** We use our scheme to simulate the classical Rossby problem, which illustrates the evolution of a simple jet-shaped initial momentum imbalance, see [6]. The initial distribution $h(x,0) \equiv 10$, $u(x,0) \equiv 0.0$ and $v(x,0) = VN_L(x)$, where

$$N_L(x) = \frac{(1+\tanh(4x/L+2)) \cdot (1-\tanh(4x/L-2))}{(1+\tanh(2))^2}, \tag{10.1}$$

and the parameters V and L are given by the Rossy number $Ro = \frac{V}{fL}$ and the Burger number $Bu = \frac{gh}{f^2L^2}$. In Figure 10.2, we use $f = 0.5$, $g = 9.81$, $Ro = 1.0$ and $Bu = 0.25$. We observe that two shocks are formed at $t/T_f = 0.6$, $T_f = 2\pi/f$, and propagate to the left and to the right from the jet, respectively. One of the shocks is formed within the jet core. The result is totally consistent with that in [6].

10.3. **A steady flow in a converging-diverging nozzle.** We use the examples in [4, Section 6.5] to test the ability of the present scheme to attain the steady state very quickly. Consider a flow in a converging-diverging nozzle, which occupies the interval $0 \le x \le 1$, and whose cross-sectional area function is given by the following expression,

$$A(x) = \begin{cases} A_{in} \exp\left(-\log(A_{in}) \sin^2(2\pi x)\right), & 0 \le x < 0.25, \\ A_{ex} \exp\left(-\log(A_{ex}) \sin^2\left(\frac{2\pi(1-x)}{3}\right)\right), \end{cases} \tag{10.2}$$

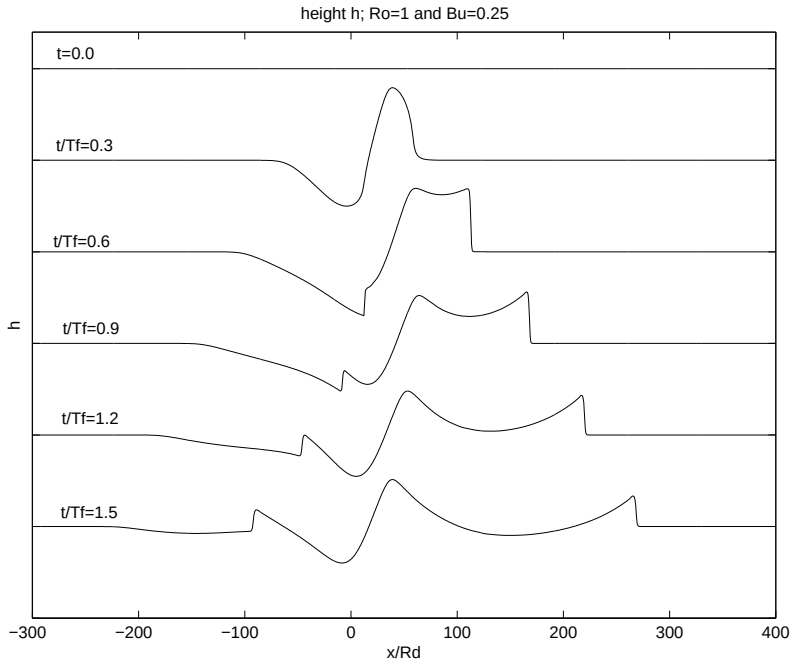

FIGURE 10.2. Shock formation from jets

where $A_{in} = 4.8643$ and $A_{ex} = 4.2346$. The initial data we use are

$$U(x,0) = \begin{cases} U_L = (\rho_0, 0, p_0), & 0 < r < 0.25, \\ \\ U_R = (\rho_0, 0, \rho_0(p_b/p_0)^\gamma), & 0.25 < r < 1, \end{cases} \tag{10.3}$$

where p_b is a constant value determined by the steady state solution at $x = 1$.

For a perfect gas with a polytropic index $\gamma = 1.4$, the Mach number $M(x) = u(x)/c(r)$ is determined by $A(r)$ through the algebraic relation

$$[A(x)]^2 = \frac{1}{[M(x)]^2}\left[\frac{2}{\gamma+2}\left(1 + \frac{\gamma-1}{2}[M(x)]^2\right)\right]^{\frac{\gamma+1}{\gamma-1}}. \tag{10.4}$$

Then the steady flow is given by

$$p(x) = p_0\left[1 + \frac{\gamma-1}{2}[M(x)]^2\right]^{-\frac{\gamma}{\gamma-1}},$$

$$\rho(x) = \rho_0\left[1 + \frac{\gamma-1}{2}[M(x)]^2\right]^{-\frac{1}{\gamma-1}}, \tag{10.5}$$

$$u(x) = M(x)\sqrt{\gamma p(x)/\rho(x)},$$

where ρ_0 and p_0 need to be specified.

We consider two cases:

(A) A smooth flow where $p(1) = 0.0272237$ is obtained from (10.5) by taking $x = 1$ in (10.4) leading to $M(1) = 3$.

(B) Setting $p(1) = 0.4$ leads to a discontinuous steady state solution, as shown by the solid lines in Figure 10.4.

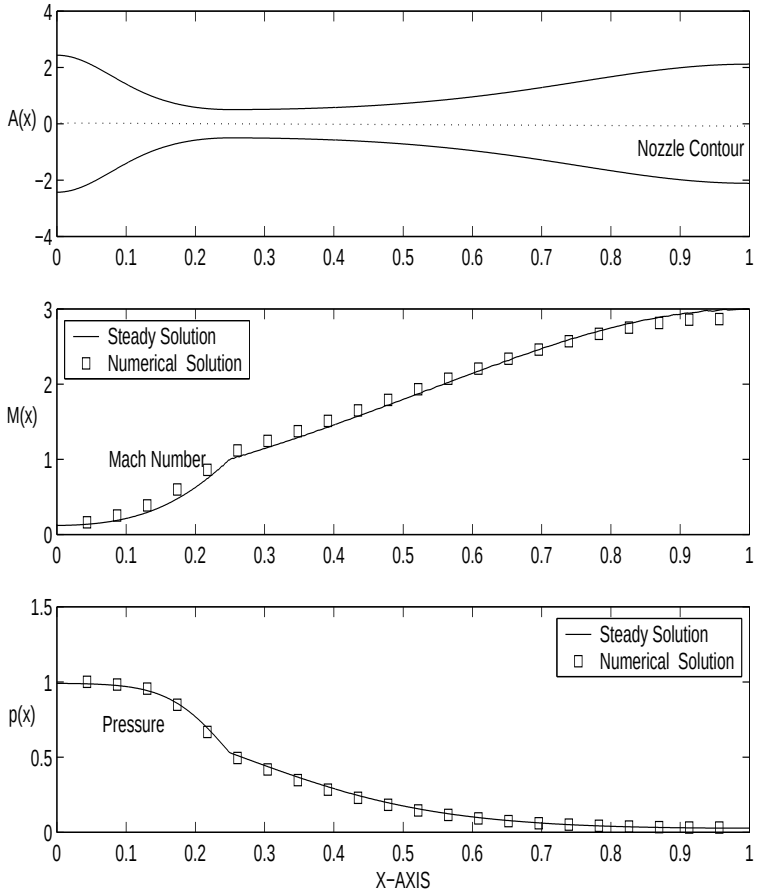

FIGURE 10.3. Large time in the Laval Nozzle. The solid line is the steady solution, and the points are the GRP solution with 22 grid points at time $t = 15.5$

We use the same strategy in [4, Section 6.5] to deal with the boundary conditions at $x = 0$ and $x = 1$. In both cases, we use 22 coarse points to display the performance of our scheme in Figures 10.3 and 10.4, and see that our GRP solution is in very good agreement with the exact solution.

In order to see how fast our GRP solution converges to the steady state, we display two different time intervals: $t = 1.0$ and $t = 2.5$, see Figures 10.5 and 10.6. It is seen that at time $t = 2.5$, our GRP solution almost attains the steady state. These show that our GRP solution can converge to the steady state very quickly.

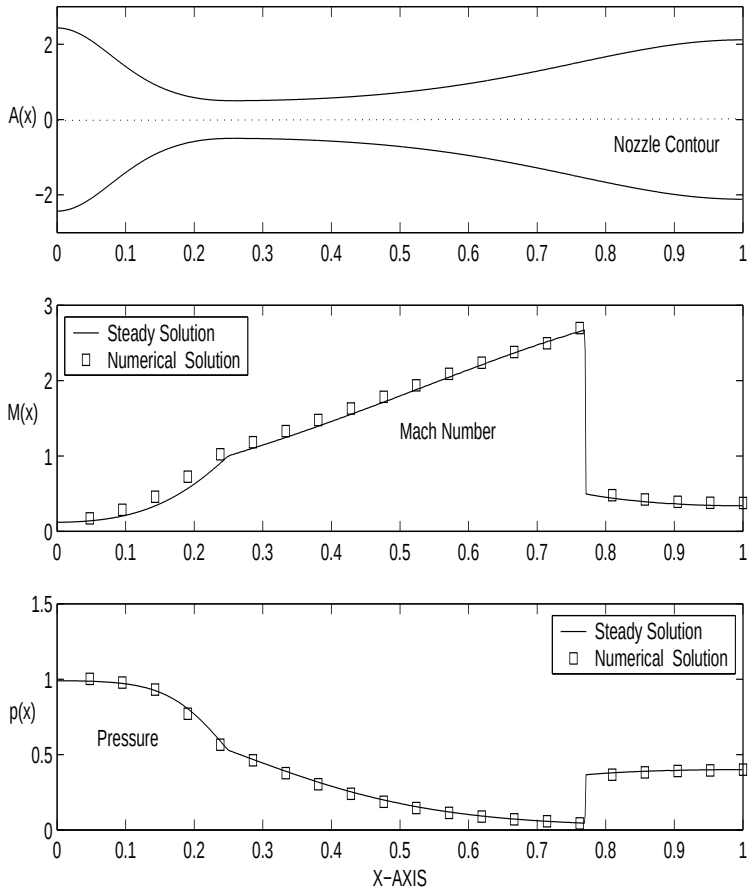

FIGURE 10.4. Large time in the Laval Nozzle. The solid line is the steady solution, and the points are the GRP solution with 22 grid points at time $t = 15.5$

ACKNOWLEDGEMENT

We would like to thank Professors J. Falcovitz, M. Lukacova, G. Warnecke and T. Zhang for their interest and many useful discussions. Matania Ben-Artzi is grateful to the Department of Mathematics, Capital Normal University for the hospitality during his visit in 2005. Jiequan Li is grateful to the Institute of Mathematics, the Hebrew University of Jerusalem for the hospitality during his visit in 2006 as well as IAN, Magdeburg University the support of Alexander von Humboldt Fundation during his stay from June 2004 to May 2005. This research is also supported by the grant NSFC with No. 10301022, the Natural Science Foundation from Beijing Municipality, Fok Ying Tong Education Foundation, the Key Program from Beijing Educational Commission with no. KZ200510028018, and Program for New Century Excellent Talents in University (NCET).

REFERENCES

[1] M. Ben-Artzi and J. Falcovitz, A second-order Godunov-type scheme for compressible fluid dynamics, *J. Comput. Phys.*, 55 (1984), no. 1, 1–32.

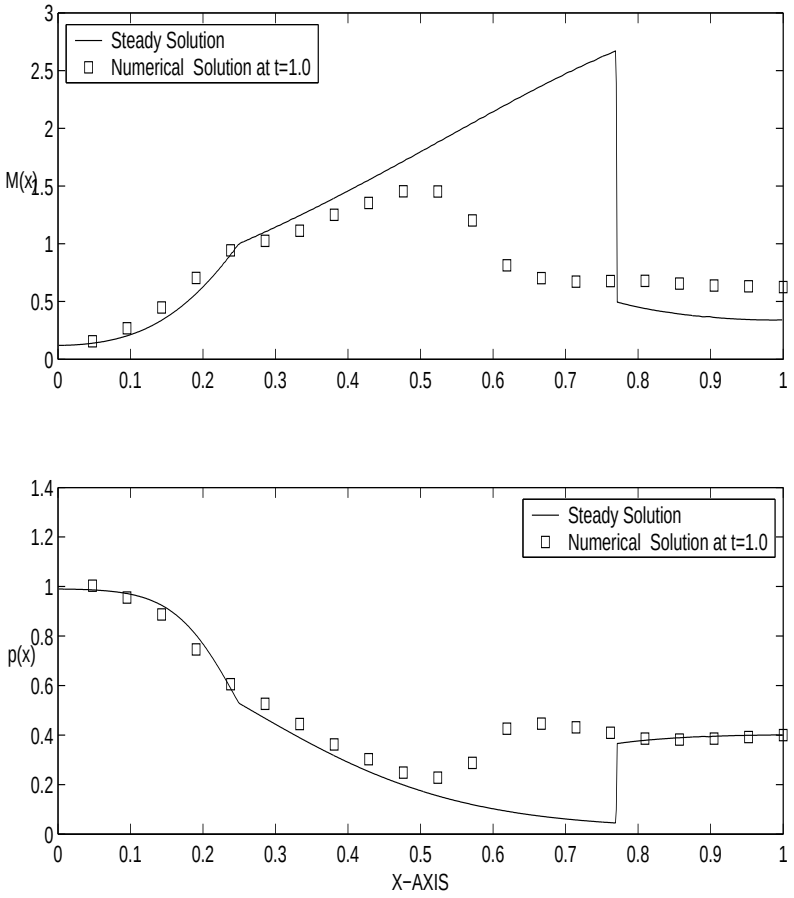

FIGURE 10.5. Large time in the Laval Nozzle. The solid line is the steady solution, and the points are the GRP solution with 22 grid points at time $t = 1.0$

[2] M. Ben-Artzi and J. Falcovitz, An upwind second-order scheme for compressible duct flows, *SIAM J. Sci. Statist. Comput.*, 7 (1986), no. 3, 744–768.
[3] M. Ben-Artzi, The generalized Riemann problem for reactive flows, *J. Comput. Phys.*, 81 (1989), no. 1, 70–101.
[4] M. Ben-Artzi and J. Falcovitz, Generalized Riemann problems in computational gas dynamics, *Cambridge University Press*, 2003.
[5] M. Ben-Artzi, J. Li and G. Warnecke, A direct Eulerian GRP scheme for compressible fluid flows, *J. Comp. Phys.*(in press), 2006.
[6] F. Bouchut, J. Le Sommer and V. Zeitlin, Frontal geostrophic adjustment and nonlinear wave phenomena in one dimensional rotating shallow water. Part 2: High resolution numerical simulations, *J. Fluid Mech.*, 514 (2004), 35–63.
[7] A. Bourgeade, Ph. LeFloch and P. -A. Raviart, An asymptotic expansion for the solution of the generalized Riemann problem. II. Application to the equations of gas dynamics *Ann. Inst. H. Poincar Anal. Non Linaire*, 6 (1989), no. 6, 437–480.
[8] C. M. Dafermos, Hyperbolic conservation laws in continuum physics, *Springer*, 2000.
[9] S. K. Godunov, A finite difference method for the numerical computation and disontinuous solutions of te equations of fluid dynamics, *Mat. Sb.* 47 (1959), 271-295.
[10] E. Godlewski and P.-A. Raviart, Numerical approximation of hyperbolic systems of conservation laws, *Applied Mathematical Sciences 118, Springer,* 1996.

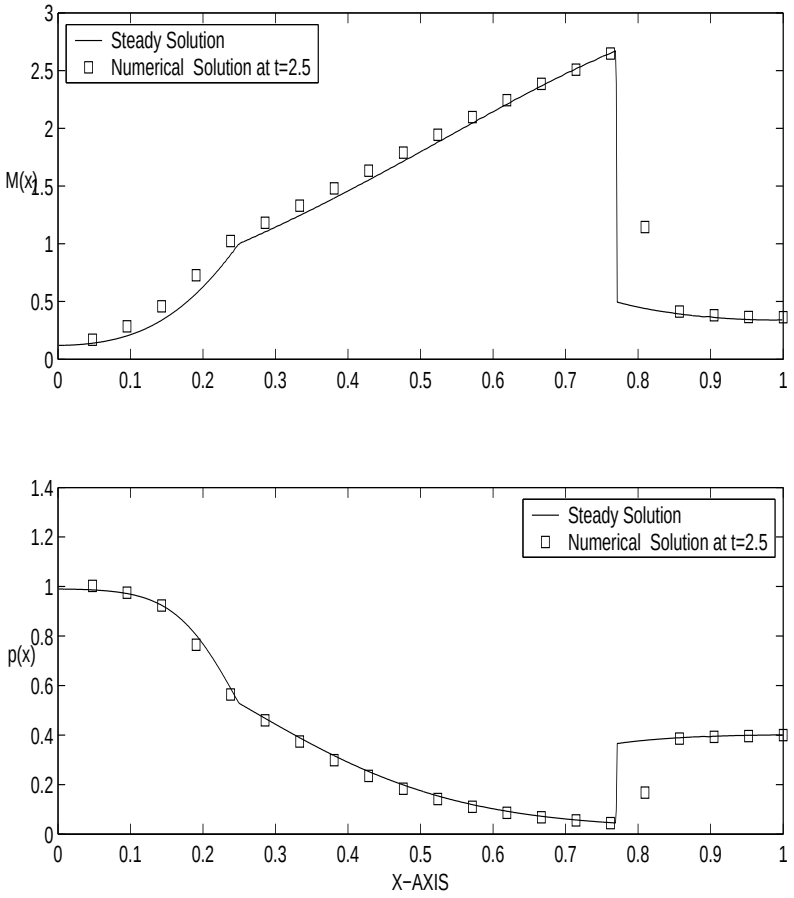

FIGURE 10.6. Large time in the Laval Nozzle. The solid line is the steady solution, and the points are the GRP solution with 22 grid points at time $t = 2.5$

[11] S. Jin, A steady-state capturing method for hyperbolic systems with geometrical source terms, *M2AN Math. Model. Numer. Anal.*, 35 (2001), no. 4, 631–645.

[12] B. van Leer, Towards the ultimate conservative difference scheme, V. A second-order sequel to Godunov's method, *J. Comput. Phys.*, 32 (1979), no. 1, 101–136.

[13] Jiequan Li and Guoxian Chen, The generalized Riemann problem method for the shallow water equations with bottom topography, *International Journal for Numerical Methods in Engineering*, Vol. 65 (2006), no. 6, 834-862.

[14] T. T. Li, Global classical solutions for quasilinear hyperbolic systems. *Research in Applied Mathematics. Chichester: Wiley. Paris: Masson.* (1994).

[15] Ph. LeFloch and P. -A. Raviart, An asymptotic expansion for the solution of the generalized Riemann problem. I. General theory, *Ann. Inst. H. Poincar Anal. Non Linaire*, 5 (1988), no. 2, 179–207.

[16] J. Smoller, Shock waves and reaction-diffusion equations, Second edition, 258.*Springer-Verlag, New York,* 1994.

[17] P. K. Sweby, High resolution schemes using flux limiters for hyperbolic conservation laws, *SIAM J. Numer. Anal.,* 21 (1984), no. 5, 995–1011.

[18] E. Toro, Riemann solvers and numerical methods for fluid dynamics. A practical introduction, *Springer-Verlag, Berlin,* 1997.

[19] E. Toro, Derivative Riemann solvers for systems of conservation laws and ADER methods, *J. Comp. Phys.*, 212(2006), 150-165.

Department of Mathematics, The Hebrew University of Jerusalem, 91904, Israel
Department of Mathematics, Capital Normal University, 100037, Beijing, P.R.China

E-mail address: Matania Ben-Artzi: mbartzi@math.huji.ac.il
Jiequan Li: jiequan@mail.cnu.edu.cn